Title
Acetylcholine acts on songbird premotor circuitry to invigorate vocal output

Permalink
https://escholarship.org/uc/item/0ms903zj

Author
Jaffe, Paul Isaac

Publication Date
2019

Peer reviewed|Thesis/dissertation

Acetylcholine acts on songbird premotor circuitry to invigorate vocal output

by
Paul I. Jaffe

DISSERTATION
Submitted in partial satisfaction of the requirements for degree of
DOCTOR OF PHILOSOPHY

in

Neuroscience

in the

GRADUATE DIVISION
of the
UNIVERSITY OF CALIFORNIA, SAN FRANCISCO

Approved:

Vikaas Sohal
_____
Vikaas Sohal
70A483C8DEB04E6...   Chair

Andrea Hasenstaub
_____
Andrea Hasenstaub

Saul Kato
_____
Saul Kato

Michael S. Brainard
_____
Michael S. Brainard
7ED6AD87FF18412...

_____
Committee Members

Acknowledgements

My advisor, Michael Brainard, essentially taught me how to be a good scientist, and deserves much of the credit for my intellectual development during the course of my Ph.D. The other members of my thesis committee(s)—Vikaas Sohal, Andrea Hasenstaub, Saul Kato, and Flip Sabes—also provided valuable feedback that substantially shaped the content of my dissertation. I must also thank all of the current members of the Brainard Lab, and many former lab members of the Doupe and Brainard Labs, for assistance in the numerous facets that make for good science: technical details, experimental design, fried-chicken and beer at the Parkside, feedback on writing and presentations, and generally good cheer. I must thank Jeff Knowles in particular for all of these things, but especially in this latter category. My family—my brother Luke, my dad David, and my mom Emily—have been unfailingly supportive throughout my Ph.D., and I have been incredibly fortunate to have them less than an hour away for the past few years. There are simply too many friends that I have leaned on to list here, but I will list most of them anyway. Ari Miller, Ilica Mahajan, Ryder Moody, Brian Basham, Robin Yeo, Sara Brockmueller, Jim Griffin, Mary Wang, and Dodd Gray: thank you, you guys rock. Last, I must especially thank Susanne Tilk, without whose companionship and support none of this would be possible.

Acetylcholine acts on songbird premotor circuitry to invigorate vocal output

Paul I. Jaffe

Abstract

The neuromodulator acetylcholine has a well-established role in enhancing sensory perception in states of heightened arousal, but whether acetylcholine acts centrally to exert an analogous influence on behavioral outputs is largely unknown. Here we use the quantifiable nature of birdsong to investigate how cholinergic tone modulates the cortical song premotor nucleus HVC, and influences vocal output. We found that dialysis of the cholinergic agonist carbachol into HVC enhanced the vigor of vocal output by increasing the pitch, tempo, amplitude and stereotypy of song. These effects did not require input from basal-ganglia circuitry, indicating direct cholinergic modulation of song premotor circuitry. Moreover, blockade of muscarinic acetylcholine receptors in HVC attenuated natural increases in vigor observed when song is directed at females in a courtship context. Neural recordings revealed that both dialysis of carbachol and courtship song were associated with higher firing rates in HVC, with conspicuous enhancement of low-frequency activity locked to the underlying rhythm of song. Further, neural activity in HVC predicted behavioral variability on a trial-by-trial basis, consistent with the possibility that natural variation in cholinergic tone influences acoustic output. Our findings establish that acetylcholine exerts a potent influence on forebrain premotor circuitry that acts to invigorate motor output, and indicates that such modulation contributes to the natural invigoration of song during courtship.

Table of Contents

List of Figures

Chapter 1: Introduction

Chapters 1, 2, and 4 describe how acetylcholine acts on the songbird premotor nucleus HVC to invigorate song, and comprise the primary body of work conducted during the course of my Ph.D. These chapters are expected to be published with minor alterations in late 2019 or early 2020. Chapter 3 describes additional analyses related to understanding the relationship between neural activity in HVC and behavioral variability. The discussion in Chapter 4 serves as a common discussion for the findings in Chapters 2 and 3.

The neuromodulator acetylcholine drives global changes in brain state as a function of arousal and vigilance (Buzsaki et al., 1988; Lee and Dan, 2012; Metherate et al., 1992). Numerous studies have demonstrated that elevated acetylcholine can act directly on cortical sensory circuitry to enhance the processing of sensory stimuli in a manner that is thought to contribute adaptively to attentional processes and heightened perceptual sensitivity (Fu et al., 2014; Herrero et al., 2008; Pinto et al., 2013). Though there are extensive cholinergic projections to motor cortical regions (Eckenstein et al., 1988; McKinney et al., 1983; Raghanti et al., 2008), there has been little attention paid to whether acetylcholine exerts analogous effects on cortical premotor circuitry during states of heightened arousal. Here we use the songbird as a model system to test whether and how acetylcholine acts on forebrain premotor circuitry to modulate movements.

Multiple lines of evidence motivate the possibility that acetylcholine acts centrally to increase 'movement vigor', which refers to the speed, amplitude, and frequency with which

1

movements are produced (Dudman and Krakauer, 2016). First, anatomical and functional studies of cholinergic neurons are consistent with the view that acetylcholine contributes to motor behavior. There are strong cholinergic projections to motor cortical regions originating from the nucleus basalis (NBM; Eckenstein et al., 1988; McKinney et al., 1983; Raghanti et al., 2008), and cholinergic neurons become more active during locomotion and other movements (Eggermann et al., 2014; Hangya et al., 2015; Nelson and Mooney, 2016; Reimer et al., 2016). Some studies that have selectively lesioned cholinergic neurons in the NBM of rats have reported abnormal reaching movements (Gharbawie and Whishaw, 2003), deficits in motor coordination (Galani et al., 2002), and reductions in swimming speed (Berger-Sweeney et al., 1994). Further, electrical stimulation of the NBM increases the amplitude and duration of vibrissae movements induced by electrical stimulation of the motor cortex (Berg et al., 2005).

Second, variation in the state of arousal is associated with variation in motor vigor. This is especially apparent for speech production, where greater arousal is associated with increases in the pitch, amplitude, and tempo of speech (Banse and Scherer, 1996; Fairbanks and Pronovost, 1938; Leinonen et al., 1997). Studies in animal models have found that greater arousal, measured by heart rate or pupil diameter, is correlated with faster reaction times (Lovett-Barron et al., 2017; McGinley et al., 2015). Similarly, numerous studies in human subjects have documented that arousing stimuli, such as unpleasant images, sudden loud noises, or cues that signal reward, can enhance the vigor of saccades, reaching movements, and forward step initiation (Bouman et al., 2015; DiGirolamo et al., 2016; Summerside et al., 2018). Consistent with this, athletes use a variety of means to increase arousal (colloquially getting 'psyched up') including listening to loud music and inhaling ammonia salts, which may enhance strength or speed in performance settings (Bartolomei et al., 2018; Bishop et al., 2009; Karageorghis et al., 1996).

Finally, diseases of the cholinergic system, such as Alzheimer's disease, are often associated with movement and speech abnormalities that can include reduced movement vigor, such as diminished grip strength, slower reaching movements, slower gait, and loss of verbal fluency (Buchman et al., 2007; Ferris and Farlow, 2013; Goldman et al., 1999). Collectively, while these observations motivate the idea that acetylcholine could modulate motor cortical regions to enhance movement vigor in states of arousal, there have been no direct tests of this possibility.

Birdsong provides a particularly attractive model for linking cholinergic modulation of premotor circuitry to movement invigoration. Song is a learned motor skill that is readily quantified with well-defined neural substrates. The forebrain premotor nucleus HVC and motor nucleus RA are essential for song adult song production, and are analogous to mammalian vocal premotor and motor cortex, respectively (Figure 2.1A). Because these structures are dedicated to song production, it is possible to manipulate and record activity at loci that are specifically linked to quantifiable behavioral output. Anatomically, HVC receives strong cholinergic innervation from the basal forebrain (Ryan and Arnold, 1981; Zuschratter and Scheich, 1990), as is the case for mammalian motor cortex (Eckenstein et al., 1988; McKinney et al., 1983; Raghanti et al., 2008). Moreover, cholinergic modulation has been shown to influence sensory responses in HVC of anesthetized birds (Shea and Margoliash, 2003), and the excitability of HVC neurons in vitro (Shea et al., 2010).

Like speech, song is naturally produced in states of greater or lesser arousal which are associated with changes in motor vigor. Male songbirds sing 'undirected' song in isolation, but also sing a 'female directed' song during courtship that is associated with greater pitch and tempo, altered song amplitude, and reduced variability from one rendition to the next (Cooper

and Goller, 2006; Hampton et al., 2009; James and Sakata, 2015; Sakata et al., 2008; Suri and

Rajan, 2018). Consistent with the notion that directed song reflects a state of greater

physiological arousal, pre-song heart rate is faster for directed song than undirected song

(Cooper and Goller, 2006). However, as in mammalian systems, the extent to which cholinergic

action on motor forebrain regions contributes to these arousal-related changes to behavior has

not been examined.

Chapter 2: Acetylcholine acts on songbird premotor circuitry to invigorate vocal output

2.1. Acetylcholine invigorates song and increases song stereotypy

To determine how acetylcholine influences song, we microdialyzed the cholinergic agonist carbachol into the premotor nucleus HVC of adult male Bengalese finches (*L. domestica*) that were signing alone ('undirected song') (Figure 2.1A; carbachol concentration 250uM – 1mM, n = 8 birds). Carbachol did not elicit gross changes to the structure of song or individual acoustic elements, referred to as 'syllables' (Figure 2.1B). However, quantitative analysis revealed a number of consistent effects that largely paralleled those observed during directed song, including an increase in pitch, amplitude, tempo, and stereotypy of acoustic structure across renditions.

To quantify effects on pitch, we identified syllables with well-defined harmonic structure and computed the normalized fundamental frequency of each syllable (drug/baseline) in a two hour period during carbachol infusion relative to a baseline period prior to drug infusion (see Methods). To control for possible circadian fluctuations in behavior (Wood et al., 2013), we compared the magnitude of changes following carbachol infusion to the magnitude of changes in response to control saline infusion, following the same procedure on alternate days. Compared to saline, carbachol elicited robust increases in pitch, comparable to pitch increases observed during directed song (Figures 2.1C and 2.1D; increase in pitch for carbachol: $1.2 \pm 0.2\%$, mean $\pm$ s.e.m.; saline: $0.3 \pm 0.1\%$; carbachol vs. saline, p = 8.8e-4, sign-rank test).

To quantify effects on song tempo, we calculated changes to the mean duration of stereotyped syllable sequences in each bird's repertoire. We found that carbachol elicited robust increases in tempo, similar to those observed during directed song (Figures 2.1F and 2.1G, decrease in sequence length for carbachol: $2.8 \pm 0.4\%$, mean $\pm$ s.e.m.; saline: $0.3 \pm 0.2\%$; carbachol vs. saline, $p = 2.4e\text{-}4$, sign-rank test).

To quantify effects on song amplitude, we averaged the smoothed amplitude envelope of each syllable over the middle 80% of the syllable (see Methods). The amplitude of individual syllables is modulated during directed song, though not always in a consistent direction (Suri and Rajan, 2018). We found that on average carbachol increased song amplitude relative to saline controls (Figures 2.1H and 2.1I; increase in amplitude for carbachol: $8.3 \pm 2.5\%$, mean $\pm$ s.e.m.; saline: $1.0 \pm 1.6\%$; carbachol vs. saline, $p = 0.012$, sign-rank test).

Increases in motor vigor have often been observed to occur in conjunction with increased stereotypy of movements in other systems (Manohar et al., 2015; Summerside et al., 2018), and across-rendition stereotypy of acoustic structure is increased during directed song. To determine if greater motor vigor is associated with increased stereotypy in song, we quantified changes to the coefficient of variation (c.v.) of pitch produced by carbachol, a measure that has been used to quantify acoustic variability in other songbird studies (Hampton et al., 2009; Kao et al., 2005). We found that carbachol produced significant increases in stereotypy, as measured by reduced pitch c.v. (Figures 2.1C and 2.1E; reduction in pitch c.v. for carbachol: $12.5 \pm 1.6\%$, mean $\pm$ s.e.m.; saline: $1.4 \pm 2.7\%$; carb vs. saline, $p = 0.0014$, sign-rank test).

We additionally tested whether carbachol dialyzed into HVC altered the sequencing of syllables. This analysis was motivated by the observation that directed songs may exhibit systematic changes in the sequencing of syllables relative to undirected songs (Sossinka and

Bohner, Hampton et al. 2009, Sakata et al. 2008). In particular, at points of sequence variability in Bengalese finch song, where a given syllable can transition to two or more subsequent syllables, the probability of transitions on average is shifted such that the more dominant transition is produced more frequently during directed song. To quantify effects on sequencing, we separately measured changes to transition probabilities induced by carbachol for two types of sequence variability: 1) 'divergent branch points', in which a given syllable transitions probabilistically to two or more different syllables (Figure S2.1A, n = 15 branch points from 7 birds) and 2) 'syllable repetitions', in which a given syllable transitions probabilistically to itself a variable number of times, before transitioning to the next syllable in song (Figure S2.1D). For 6 out of 15 divergent branch points, carbachol significantly affected transition probabilities, while only one of these branch points changed significantly following saline infusion ($p<0.05$, generalized likelihood ratio test for homogeneity; Methods, Figure S2.1B). Additionally, the average magnitude of change in transition probability for carbachol experiments was significantly larger than for saline control experiments (Figure S2.1C). For syllable repetitions, carbachol produced a significant increase in the number of times a syllable was repeated in succession before transitioning to the next syllable, as is the case for directed song (Figure S2.1E, $p = 0.031$, two-sided sign-rank test, n = 6 birds, 7 repeat syllables). Moreover, more variable repeat sequences were more affected by carbachol, as has been observed for temperature manipulations of HVC (Figure S2.1F, Zhang et al., 2017). Hence, carbachol dialyzed into HVC caused significant changes to aspects of sequence variability that are also affected by social context, and in the case of syllable repetitions caused a significant shift towards more stereotyped sequences (greater number of repetitions) as is observed in directed song.

Next, we investigated the pharmacology underlying cholinergic modulation of song. Carbachol acts on both major classes of acetylcholine receptor (muscarinic and nicotinic), and both classes of receptors are expressed in HVC (Asogwa et al., 2018; Ball et al., 1990; Watson et al., 1988). To determine if the behavioral effects of carbachol were mediated by one or both classes of receptors, we microdialyzed carbachol in combination with antagonists of either muscarinic or nicotinic receptors into HVC (n = 5 birds). For pitch, pitch c.v., and amplitude, we found that the effect produced by carbachol was blocked by the muscarinic antagonist atropine (500uM-2mM) but not by the nicotinic antagonists MEC and MLA (MEC: 400uM, MLA: 100uM; Figures 2.1D, 2.1E and 2.1I). For tempo, we observed a non-significant trend toward attenuation by atropine compared to MEC+MLA (Figure 2.1G). These data indicate that activation of muscarinic receptors is largely responsible for the invigoration of acoustic parameters of song syllables by carbachol.

2.2. Acetylcholine invigorates movement via the motor pathway

In principle, acetylcholine could act to invigorate song through either of two major pathways emanating from HVC: the motor pathway, via a direct projection from HVC to RA, or through basal ganglia circuitry via an indirect pathway from HVC->Area X->DLM->LMAN->RA (the Anterior Forebrain Pathway or 'AFP', Figure 2.2A). Previous studies in mammalian systems have identified the basal ganglia as a key locus for the modulation of motor vigor (Panigrahi et al., 2015; Yttri and Dudman, 2016), supporting the possibility that the effects of carbachol infusion into HVC could reflect primarily an influence on AFP circuitry. Further, a number of studies in songbirds have identified the AFP as a critical site for social modulation of pitch variability that occurs during directed song (Hampton et al., 2009; Kao and Brainard, 2006;

Kao et al., 2005; Stepanek and Doupe, 2010), and electrical microstimulation within the AFP output nucleus LMAN can elicit acute changes to pitch and amplitude (Kao et al., 2005).

To determine whether basal ganglia circuitry contributes to the acoustic changes produced by carbachol, we microdialyzed carbachol into HVC while inactivating LMAN with muscimol (Figure 2.2A, n = 4 birds). LMAN is the main output nucleus of the AFP, and muscimol inactivation of LMAN disconnects the AFP from the song motor pathway. As in previous studies, infusion of muscimol caused a significant decrease in pitch variability, confirming that LMAN was effectively inactivated (Figure 2.2F). However, even when LMAN was inactivated in this fashion, infusion of carbachol into HVC caused increases in pitch, amplitude, tempo, and song stereotypy (Figures 2.2B-2.2F). For all of these features, the increases produced by the combined carbachol + LMAN inactivation condition were greater than changes produced by LMAN inactivation alone (p < 0.05 for pitch, amplitude, and tempo; p = 0.084 for pitch c.v.; sign-rank test). Moreover, for each feature, the sum of changes elicited by carbachol and LMAN inactivations individually was not significantly different from the combined carbachol + LMAN inactivation condition (p > 0.05 in each case, sign-rank test). These results indicate that increased cholinergic tone in HVC modulates song via primary motor circuitry independently of input from the songbird basal-ganglia.

2.3. Acetylcholine increases neural activity in HVC

To further understand the mechanism by which acetylcholine influences behavior, we recorded multi-unit neural activity in HVC of singing Bengalese finches before and after microdialysis of carbachol (Figure 2.3A). We focused on recording multi-unit activity, since stable recordings of isolated single units are difficult to maintain for multiple hours in

conjunction with pharmacological manipulations, as required for these experiments. Following microdialysis of carbachol, we observed that the pattern of neural modulation with respect to song features was largely preserved (Figure 2.3B and S2.2): the mean correlation coefficient between syllable-aligned firing rates before and after carbachol was 0.92 (0.92 ± 0.0098, mean ± s.e.m., n = 202 multi-unit sites x syllables, 26 unique multi-unit sites, 5 birds). The similarity in firing patterns before and after carbachol is consistent with the absence of gross disruptions to song, and demonstrates that our recording sites were largely stable for the duration of the experiment.

To determine if acetylcholine had a net suppressive or excitatory effect on HVC activity, we computed trial-averaged firing rates aligned to syllable onsets, for each multi-unit site and syllable (Figure 2.3B and S2.2). Averaging across all sites and syllables, we found that carbachol increased multi-unit firing rates in HVC relative to baseline (Figure 2.3C). In contrast, saline control experiments had no effect on HVC firing rates (Figure 2.3D). To quantify the magnitude of this effect, we calculated the difference in firing rate between carbachol and baseline in different windows around syllable onsets (Figure 2.3E). We found that the increase in firing rate elicited by carbachol was significantly greater than that produced by saline in both a 30ms window preceding syllable onsets, and a 30ms window just after syllable onsets (p < 5e-4 in both cases, rank-sum test). Similar results were obtained for a range of different windows.

The reduction in behavioral variability we observed during microdialysis of carbachol led us to consider the possibility that this was caused by a corresponding reduction in neural variability in HVC. To evaluate this, we measured the Fano factor (across-trial spike count variance/mean spike count) for each multi-unit site and syllable, in different windows around syllable onsets (Figure 2.3F). On average, the change in Fano factor produced by carbachol was

not significantly different from that produced by saline (p = 0.92, 30ms window prior to syllable onsets; p = 0.15, 30ms window after syllable onsets, rank-sum test). We also evaluated neural variability by calculating the spike count variance. We found no significant difference between carbachol and saline in the window prior to syllable onsets (p = 0.38, rank-sum test), and observed a slight tendency for carbachol to increase neural variability in the window after syllable onsets (p = 0.037). As such, we did not find evidence to support the possibility that the reduction in behavioral variability was caused by reduced neural variability in HVC.

In general, the firing rate changes elicited by carbachol were complex, and varied in magnitude relative to acoustic features of song (Figure 2.3B and S2.2). Nonetheless, we considered whether simple transformations of the baseline firing rate function could account for the observed firing rate changes. For each syllable-aligned firing rate function, we evaluated how well the change produced by carbachol was captured by an additive model, in which the baseline firing rate was shifted up or down by a constant amount, and a multiplicative model, in which the baseline firing rate was multiplicatively scaled by a constant amount (see Methods). Consistent with our qualitative observations, both models failed to account for the data in the vast majority of cases. We evaluated how well each model described the change in firing rate by a relative distance index that quantifies the how far the best-fitting model is from the carbachol rate function, relative to the distance between the baseline and carbachol rate functions (see Methods, referred to as 'distance index'). For this index, which ranges from zero to one, a value of one indicates that the best-fit model fully captures the transformation produced by carbachol, while a value of zero indicates that none of the transformation has been accounted for. Across multi-unit sites and syllables, the median of the distance index was 0.41 for the additive model, and 0.42 for

the multiplicative model, indicating that both models accounted for less than half of the firing rate change produced by carbachol in the majority of cases.

Despite this apparent complexity, we observed a tendency for carbachol to produce greater firing rate increases prior to syllable onsets than within the syllable (Figures 2.3C and 2.3E). In the 100ms window around syllable onsets, the increase in firing rate produced by carbachol exhibited a sharply-peaked maximum of 33Hz at -25ms relative to syllable onsets, and a minimum of 13Hz at 14ms. Additionally, the firing rate increase produced by carbachol was significantly greater in the 30ms window preceding syllable onsets than in the 30ms window just after syllable onsets (Figure 2.3E, $p = 1.1e-4$, sign-rank test). In summary, we found that carbachol had a net excitatory influence on population-level activity within HVC, and tended to differentially increase firing rates relative to syllable onsets.

2.4. Acetylcholine enhances low-frequency rhythmic activity in HVC

The observation that carbachol preferentially increases activity prior to syllable onsets led us to conduct a more detailed set of analyses relating the firing rate changes elicited by carbachol to the underlying rhythm of song. Previous analyses of zebra finch song have found that both the song amplitude envelope and HVC population activity exhibit a slow rhythmic modulation in the 5-10Hz range, with HVC activity peaking ~20ms prior to syllable onsets and reaching a minimum ~20ms prior to syllable offsets (Lynch et al., 2016; Saar and Mitra, 2008). Consistent with these prior observations, we found that population-level activity in HVC of Bengalese finches was rhythmically modulated relative to syllable onsets (Figures 2.3C and 2.3D).

To relate the firing rate changes elicited by carbachol to the underlying rhythm of song, we calculated the population average spectrum of multi-unit spike trains before and after

carbachol (Figures 2.4A, 2.4B and S2.3A; n = 25 multi-unit sites from 5 birds). Spike train

spectra were computed after aligning trials to the onset of stereotyped sequences of syllables

from each bird's song (see Methods). We observed a broad peak in the 5-10Hz range of the

population average spike train spectrum, similar to previous reports in zebra finches (Lynch et

al., 2016). Further, each bird exhibited a peak in the coherence between population spike trains

and song amplitude in the 5-10Hz range (Figure S2.3C, max at 6.3Hz, averaged across 5 birds).

Interestingly, we found that carbachol preferentially increased power at frequencies

below 10Hz (Figures 2.4A and 2.4B), a pattern we observed in four out of five birds (Figure

S2.3A). Averaged across recording sites, carbachol produced a significant increase in power in

the 0-10Hz range relative to baseline (p = 1.6e-4, sign-rank test; mean ± s.e.m. increase in power

of 24 ± 6.3%; n = 25 multi-unit sites from 5 birds). In contrast, we did not observe a significant

increase in power for saline control experiments in this frequency range (Figure 2.4C and S2.3B;

p = 0.79, sign-rank test; mean ± s.e.m. increase in power of 1.5 ± 6.4%; n = 12 multi-unit sites

from 4 birds). The magnitude of increase in power in the 0-10Hz range was also significantly

greater for carbachol than for saline controls (p = 0.034, rank-sum test). Thus, carbachol

preferentially enhances spiking activity at frequencies corresponding to the underlying rhythm of

song.

2.5. Acetylcholine contributes to the social modulation of song

The influence of cholinergic modulation on undirected song (produced by males singing

in isolation) parallels changes to song that are elicited by introduction of a female in a courtship

context (directed song). This similarity prompted us to wonder if cholinergic signaling in HVC

contributes to social modulation of song. To investigate this possibility, we microdialyzed either

saline or the muscarinic antagonist atropine into HVC while birds sang directed and undirected

song during interleaved sessions (Figure 2.5A). Different conditions (saline vs. atropine), were tested on different days in the following order: saline pre, atropine, and saline post (Figure 2.5B). We measured the magnitude of social modulation of song features by computing a normalized quantity (directed/undirected) for each feature. As previously reported (Hampton et al., 2009; James and Sakata, 2015; Sakata et al., 2008), directed song was faster, more stereotyped, and higher in pitch than undirected song (Figures 2.5D - 2.5F, saline conditions). We found that atropine significantly attenuated the social modulation of pitch c.v. and pitch (Figures 2.5C- 2.5E). In contrast, we did not find significant attenuation of the increase in song tempo, though small sample and effect sizes may have precluded our ability to detect a significant effect (Figure 2.5F). Importantly, while pitch and pitch c.v. effects were attenuated by atropine, pitch, pitch c.v., and tempo were all still significantly modulated by social context ($p < 0.05$ in each case, sign-rank test). The observation that these features still exhibited some degree of social modulation with atropine argues against a non-specific impairment of perceptual processes that are required to engage in directed song (for example, an inability to recognize the presence of a female).

In principle, an attenuation by atropine of the differences between directed and undirected song could reflect an influence of atropine on songs produced in either, or both, of the social contexts. When we examined the data split by condition (directed vs. undirected), we found that atropine had a significant effect in decreasing the stereotypy of directed song (towards the greater variability normally present in undirected song), but had no effect on the variability of undirected song (Figure S2.4A). Similarly, the mean pitch of directed, but not undirected songs, was significantly lower with atropine compared to the saline pre and post conditions (Figure S4B). No significant differences in song tempo were observed between conditions for either

directed or undirected songs (Figure S2.4C). The specific effects of atropine that we observed on directed but not undirected song argues for the attenuation of a process that is actively engaged during directed song, rather than an effect primarily on undirected song. Thus, these results indicate that activation of muscarinic receptors in HVC during natural conditions of heightened arousal contributes to the increased pitch and reduced pitch variability of directed song.

2.6. HVC activity is modulated by social context

The finding that cholinergic signaling within HVC contributes to social modulation of song led us to wonder if directed song and microdialysis of carbachol elicit similar changes to HVC activity. To determine how social context influences HVC activity, we used a similar multi-unit recording approach to that which we had deployed to assess the influences of carbachol on HVC activity; however, instead of pharmacological manipulations we varied the social context in which bird's sang during interleaved recording sessions (Figure 2.6A, n = 5 birds). While previous neural recordings within HVC have not found conspicuous social modulation of neural activity in HVC_X projection neurons, differences in IEG expression within HVC have been reported (Matheson et al., 2016), suggesting some degree of modulation by social context, possibly restricted to the other cell classes within HVC (the HVC_{RA} projection neurons and HVC interneurons). We therefore focused on recording multi-unit activity, which should sample from all cell classes within HVC.

To determine how social context influences multi-unit firing rates within HVC, we computed trial-averaged firing rates aligned to syllable onsets separately for directed and undirected trials. As observed after microdialysis of carbachol, we found that the pattern of neural modulation with respect to song features was largely conserved across social contexts: the

mean ± s.e.m. correlation coefficient between directed and undirected firing rates was 0.90 ± 0.010 (Figure 2.6B and S2.5, n = 151 multi-unit sites x syllables, 15 unique multi-unit sites, 5 birds). While firing patterns across social contexts were largely similar, we found that multi-unit firing rates were consistently higher during directed song, as observed after microdialysis of carbachol (Figures 2.6B, 2.6C, 2.6D and S2.5). A raster plot and smoothed firing rates for one example site are shown in Figure 2.6B. For this site, directed song was associated with a consistent increase in activity, as revealed by calculating mean firing rates for each block of directed or undirected trials (Figure 2.6B, bottom panel; additional examples in Figure S2.5).

The magnitude of firing rate increase and pattern of modulation observed during directed song were similar to that produced by carbachol. Firing rates during directed song were significantly greater than undirected song in both a 30ms window prior to syllable onsets and a 30ms window just after syllable onsets (Figure 2.6D, p < 1e-9 in both cases, sign-rank test). For both time windows, the magnitude of firing rate increase observed during directed song was not significantly different from that observed during microdialysis of carbachol (p > 0.05 in both cases, rank-sum test; -30 to 0ms window: mean ± s.e.m. firing rate increase of 27 ± 3.8Hz for carbachol, 27 ± 3.7Hz for directed; 0 to 30ms window: 18 ± 3.4Hz for carbachol, 18 ± 2.1Hz for directed). As for carbachol, we found that the magnitude of firing rate increase was significantly greater in the window prior to syllable onsets than after syllable onsets (Figure 2.6D, p = 0.011, sign-rank test). In the 100ms window centered on syllable onsets, the average firing rate difference exhibited a maximum of 32Hz at -21ms, and a minimum of 8.2Hz at 34ms. We also determined if the firing rate transformation observed during directed song could be explained by either an additive or multiplicative scaling of the undirected firing rate function (see Methods). In good agreement with the complex firing rate changes observed during carbachol, both additive

and multiplicative models yielded poor descriptions of the firing rate transformation observed during directed song. The median distance index (see Methods) used to evaluate how well these models explained the change in firing rate was 0.269 for the additive model, and 0.268 for the multiplicative model, indicating as for carbachol that both models accounted for less than half of the firing rate change observed during directed song in the majority of cases.

Since we observed that carbachol enhanced spiking activity at lower frequencies (0-10Hz), we determined if directed song was similarly associated within enhanced spiking activity at frequencies corresponding to the underlying rhythm of song. Indeed, we found that directed song was associated with strong enhancement of spiking activity at lower frequencies (Figure 2.6E and S2.6). Averaged across recording sites, we observed a significant increase in power in the 0-10Hz range relative to undirected song ($p = 0.022$, sign-rank test; mean $\pm$ s.e.m. increase in power of $22 \pm 11\%$; $n = 13$ recording sites from 5 birds). The magnitude of this increase in power during directed song was not significantly different from that observed during microdialysis of carbachol ($p = 0.62$, rank-sum test). In summary, we discovered a previously unknown influence of social context on HVC spiking activity, namely that population-level activity is greater during directed song than undirected song. Further, we observed that the pattern and magnitude of neural modulation for microdialysis of carbachol and social modulation of song were similar, supporting the view that acetylcholine drives increased motor vigor by mechanisms that are naturally engaged in a state of behavioral arousal.

2.7. Methods

Statistics.

Unless noted otherwise, we used non-parametric two-sided tests for comparing two samples: the Wilcoxon rank-sum test for unpaired data and the Wilcoxon signed-rank test for paired data. Details for all statistical tests are included in the figure legends and/or the main text. For all tests, we rejected the null hypothesis if $p < 0.05$. No statistical methods were used to predetermine sample sizes, though our sample sizes are comparable to those used in previous publications (Sakata and Brainard, 2008; Sober et al., 2008; Stepanek and Doupe, 2010). Unless noted otherwise, data collection and analysis were not performed blind to experimental conditions. Details on randomization of conditions are discussed in the relevant methods section where applicable. A small number of syllables with very low sample sizes were excluded; details are given in the corresponding methods section. For pitch, tempo, and amplitude measurements, a simple heuristic was used to remove outliers (described in detail below). For amplitude analyses, we excluded a small number of experiments (3/75, combined across conditions) in which large (>25%) and sudden changes in amplitude occurred, as these were likely caused by the bird changing its orientation with respect to the recording microphone (described in detail below). All analyses were performed using custom-written MATLAB (Mathworks) software.

Subjects. Data were collected from 25 adult male Bengalese finches (*Lonchura striata domestica*; microdialysis only: n = 15; microdialysis + electrophysiology: n = 5; electrophysiology only: n = 5). Two birds with indeterminate ages were obtained from outside vendors (n = 1) or other songbird labs (n = 1); these birds had adult-like song and physical characteristics. All other birds were bred in the University of California, San Francisco (UCSF)

breeding facility. The ages of these birds ranged from 124 to 239 days at the start of experiments. Adult female Bengalese finches (>120 days old) were used to obtain directed song. During experiments, male birds were individually housed in sound-attenuating chambers (Acoustic Systems) on a 14h:10h light:dark cycle with food and water provided ad libitum. All procedures were performed in accordance with protocols approved by the UCSF Institutional Animal Care Use Committee.

Song recording. Audio was recorded in a custom-written Labview program (National Instruments; digitized at 32kHz) using an omnidirectional lavalier microphone (Countryman), or with a USB interface board (Intan; digitized at 30kHz) using a custom-made microphone and pre-amplifier system.

***In vivo* microdialysis.**

Guide cannulae (CMA 7, CMA Microdialysis) were implanted into HVC or both HVC and LMAN using stereotaxic coordinates. For combined electrophysiology/microdialysis experiments, cannulae were implanted unilaterally in the left HVC (n = 5 birds). For all other experiments, cannulae were implanted bilaterally (HVC + LMAN: n = 4 birds; HVC only: n = 11 birds). After birds recovered from surgery, we inserted microdialysis probes into the cannulae (CMA 7; 0.24-mm diameter, 1-mm diffusion membrane, 6-kDa diffusion pore size).

Dialysis probes were connected to fluid pumps through flexible tubing. In some cases, a fluid switch (BASi Uniswitch) was used to switch between solutions; otherwise, solutions were exchanged by hand. Outflow was continually monitored throughout the duration of the experiment. In some cases, we observed leakage from the dialysis tubing or diminished flow as

indicated by the volume of the outflow. These experiments were excluded from summary analyses and dialysis probes were replaced for subsequent experiments. For the baseline period of an experiment, we infused saline at a rate of 1-1.5uL/min. For experiments without combined electrophysiology, solutions were exchanged to either saline (for control experiments) or drug (carbachol, muscimol, etc.) after 2-3 hours. To control for possible circadian fluctuations in behavior, solutions were exchanged at the same time each day across experiments. For experiments with combined electrophysiology, the exact duration and time of day that solutions were exchanged varied depending on when the bird sang. For animals in which we tested multiple different conditions (e.g., carbachol vs. carbachol + atropine), each condition was repeated a variable number of times on different days in a randomized order. At least one full day of saline-only infusion was allowed between consecutive drug infusion experiments.

In a subset of animals we conducted a series of pilot experiments to determine effective drug concentrations. For carbachol experiments, we increased the concentration of carbachol until a clear pitch effect was observed, up to a maximum concentration of 1mM. In one case, the initial concentration of carbachol (500uM) caused the bird to call continuously and was reduced on subsequent experiments to 250uM. For LMAN inactivation experiments, we increased the concentration of muscimol until a clear reduction in pitch c.v. was observed, or reduced the concentration if birds did not sing. For combined microdialysis and electrophysiology experiments, no pilot experiments were conducted and all experiments were conducted at a concentration of 1mM. Pilot experiments were not included in summary analyses. No formal procedure was used to establish effective concentrations of the acetylcholine receptor antagonists; we included all experiments conducted at the highest concentration. The final concentration of drugs used in this study is as follows. Carbachol (Santa Cruz Biotechnology):

250uM-1mM; muscimol (Tocris): 250uM-1mM; mecamylamine hydrochloride (Sigma): 400uM; atropine sulfate (Sigma): 500uM-2mM; methyllycaconitine citrate salt (Sigma): 100uM.

In vivo electrophysiology.

For experiments in which we combined electrophysiology with microdialysis (n = 5 birds), extracellular recordings from HVC were obtained with custom-designed commercial tungsten electrode arrays (MicroProbes, 6MOhm electrode impedances, n = 1 bird), multi-site silicon electrode arrays (NeuroNexus, A4x4-3mm-50-125-413-H16_21mm, n = 1 bird), or custom-designed tungsten electrode arrays assembled in-house (FHC or MicroProbes, electrode impedances ranged from 0.5MOhm to 10MOhm, n = 3 birds). Electrode arrays were positioned using a custom hand-driven microdrive.

For all other experiments, recordings were obtained with tungsten electrode arrays assembled in-house (MicroProbes, electrode impedances were 0.5MOhm for multi-unit recordings and 5-6MOhm for single-unit recordings). Electrode arrays were positioned using a custom hand-driven microdrive, or a custom motorized microdrive (Faulhaber motor, n = 1 bird).

Neural data were amplified, band-pass filtered (1-7500Hz), and digitized (30kHz) with a commercially available head-mounted amplifier board (Intan Technologies, RHD2216) or a custom amplifier board designed in-house to reduce weight, made with the RHD2216 amplifier chip (Intan Technologies). Neural and audio data were registered with a USB interface board (RHD2000, Intan Technologies).

Directed song. For experiments in which we microdialyzed atropine (Figures 2.5 and Figure S2.4), we collected directed song on three separate days, with sessions separated by one day (day

1: saline, day 3: atropine, day 5: saline; see Figure 2.5B). For each session, females were

presented 30 or 40min. apart in a cage placed next to the male's cage (time constant across

sessions for a given bird), for a total of 2 minutes for each presentation. For a given male bird,

the same sequence of females was presented in the same order across sessions. The presence of a

courtship dance was used to confirm that males sang directed song (puffing of feathers,

orientation toward female, and hopping from side-to-side). For experiments in which we

recorded neural activity during manipulation of social context, females were presented 15-

20min. apart in a cage next to the male's cage, or were introduced directly into the male's cage.

Analysis of song features.

Definition of analysis windows. To quantify the behavioral effects of carbachol (Figures 2.1 and

S2.1), we used an analysis window of 1 to 3h after estimated time of drug delivery into the brain

(drug analysis window). This same choice of analysis window was used for all animals and

experiments, and for all reported behavioral features. Baseline measurements were calculated

from a 1 to 2h window prior to drug onset (baseline analysis window).

For experiments in which we probed the requirement of LMAN for the behavioral effects

of carbachol (Figure 2.2), we determined the onset of drug effects for the carbachol and

muscimol conditions by visual assessment of the raw pitch values. The onset of the drug analysis

window was defined as the maximum of the estimated carbachol and muscimol onsets. The

offset of the drug window was defined as 1 hour after the onset. This procedure ensured that both

drugs would be active during the combined carbachol + muscimol condition. The baseline

analysis window was defined as described above.

For social context experiments (Figures 2.5 and S2.4), we analyzed all directed songs and a random subset of interleaved undirected songs.

Pitch and pitch variability. Songs were segmented into syllables based on amplitude threshold crossings. A random subset of syllables with clear harmonic structure were manually labelled and used in subsequent analysis. To quantify the pitch of a given syllable rendition, raw audio data was bandpass filtered between 500 and 10,000Hz, and a spectrogram was computed using a gaussian-windowed (σ = 1-3ms) short-time Fourier transform (window size = 1024 samples; overlap = 1020 samples). From the spectrogram, a pitch contour was calculated by finding the maximum power in a frequency range around the first harmonic in each time bin, followed by parabolic interpolation of the resulting time series. The pitch of the syllable was then determined by averaging the pitch contour across a constant frequency component of the syllable. The coefficient of variation of pitch (pitch c.v.) was computed as the standard deviation divided by the mean. For a given experiment, we excluded pitch measurements that exceeded four times the median absolute deviation from the median, repeating this process three times. This procedure functions as a simple heuristic for culling measurements resulting from incorrect segmentation of the amplitude envelope. We excluded syllables with fewer than 15 trials in either the baseline or drug periods. This criterion was applied after outlier removal.

For social context experiments, the accuracy of each pitch calculation was confirmed by visual assessment of the pitch contour overlaid on the syllable spectrogram, and inaccurate pitch calculations (due to incorrect segmentation, for example) were excluded from summary analyses. Exclusions were performed blind to social context condition (directed vs. undirected). No additional outlier removal was performed.

Song tempo. For each bird, we identified one or two stereotyped syllable sequences of syllables and determined the duration of the sequence from the onset of the first syllable in the sequence to the onset of the last syllable in the sequence. Syllable onsets were determined by an amplitude threshold and were used for tempo measurements because they were more sharply defined than offsets. Outlier removal was performed as described for pitch measurements. As for pitch, we excluded syllable sequences with fewer than 15 trials in either the baseline or drug periods.

Amplitude. Amplitude for a given syllable was calculated by averaging the smoothed amplitude envelope over the middle 80% of the syllable. Amplitude envelopes were calculated by bandpass filtering the raw audio signal between 500 and 10,000Hz (80th order linear-phase FIR filter), computing the root-mean-square, and smoothing with a sliding 2.5ms rectangular window. Outlier removal was performed as described for pitch measurements, and syllables with fewer than 15 trials in either the baseline or drug periods were excluded. In a small number of experiments, we observed large (>25%) and sudden changes in amplitude that were likely caused by the bird changing its orientation with respect to the recording microphone. We excluded these experiments if the mean amplitude for each syllable changed by more than 25% in the drug period relative to the baseline period (3/75 experiments excluded, combined across conditions).

Repeat syllables. Syllables that repeated a variable number of times were classified as repeat syllables, with the following exceptions: syllables that repeated only once or twice were considered as branch points (see below). We also did not consider high entropy syllables that sometimes separate motifs in Bengalese finch song as repeat syllables, since these are difficult to

distinguish from introductory notes. Syllables separated by a gap of more than 200ms were not considered a part of the same repeat sequence. The primary cohort of animals used in this study had few repeat syllables and so we included an additional cohort of animals that did not have paired saline control experiments (n = 4 additional animals).

Prior to statistical comparisons and calculation of normalized repeat length, we pooled repeat counts for experiments with the same condition. Repeat length c.v. was calculated from the pooled repeat length distributions from the pre period of all carbachol experiments.

Branch points. A syllable that transitions probabilistically to two or more syllables is a branch point (specifically, a divergent branch point). Similar to previous studies (Zhang et al., 2017), we treated sequences of repeating syllables as a single song element. Syllables separated by a gap of more than 200ms were not included in the calculation of transition probabilities.

To determine if transition probabilities at a given branch point were significantly different in the baseline and drug windows, we employed a generalized likelihood ratio test for homogeneity of transition probabilities. Specifically, we test the null hypothesis H_0: $p_i = q_i$ for all $i = 1,\dots k$; where p_i denotes the probability of transition i in the baseline period, and q_i denotes the probability of transition i in the drug period. The test statistic is the likelihood ratio $L(M_{sub})/L(M_{full})$, where M_{full} denotes a multinomial probability distribution with parameters determined from the combined (baseline+drug) dataset by maximum likelihood, and M_{sub} denotes two multinomial models with parameters determined from the segregated baseline and drug period datasets. Intuitively, this ratio captures the extent to which a single multinomial model is a better descriptor of the data than two separate multinomial models split by baseline and drug periods, thereby adjudicating the hypothesis that transition probabilities have changed.

Determining differences between carbachol and saline based on the fraction of significant cases is potentially confounded if there are systematic differences in sample sizes between the two data sets. However, sample sizes did not differ significantly between baseline and drug periods ($p = 0.89$, two-tailed sign-rank test; mean sample sizes for combined baseline+drug periods: carbachol, $n = 450$ transitions; saline, $n = 528$ transitions).

The magnitude of change in transition probability was calculated as the summed change in transition probability for the first $n-1$ of n possible transition types at that branch point (Figure S2.1C). Prior to calculating this statistic, we combined data from all baseline or drug windows of a given condition.

Neural analyses

Spike sorting

Multi-unit activity was extracted using the free software Wave clus (Quiroga et al., 2004). Briefly, raw voltage traces were band-pass filtered between 300 and 4000Hz. Events greater than 3.5 and below 50 times the standard deviation of the median noise level in the negative direction were considered spikes, with a minimum refractory period between events of 0.2ms.

Analysis of firing rates and neural variability

Trial-averaged firing rates before and after carbachol/saline, and for directed and undirected song, were calculated by aligning spike trains to syllable onsets and convolving with a 5ms s.d. gaussian kernel. Firing rate differences elicited by carbachol or directed song were calculated by averaging smoothed firing rates over a 30ms window just prior to syllable onsets, and a 30ms window just after syllable onsets. The Fano factor was calculated as the across-trial spike count

variance divided by the mean spike count in these same time windows relative to syllable onsets. For all analyses, site/syllable pairs with fewer than 10 trials or firing rates less than 50Hz in either the baseline/undirected or drug/directed periods were excluded. The minimum firing rate criterion was applied to a 100ms window centered at the onset of the syllable.

Spectral analysis of song amplitude and multi-unit activity

Multi-unit spike train power spectral densities (PSDs) and coherence between song amplitude and spike trains were computed using code available from the Chronux package (Lynch et al., 2016; Mitra and Bokil, 2007). Spike trains and amplitude envelopes were aligned to the onset of stereotyped sequences of syllables from each bird's song (range: 4 to 9 syllables). As for our other neural analyses, we excluded experiments with fewer than 10 trials or firing rates less than 50Hz in either the baseline/undirected or drug/directed periods. Firing rates used for the 50Hz exclusion criterion were calculated over the entire duration of the stereotyped syllable sequence used for spectral analysis.

Evaluating additive and multiplicative models

For each multi-unit site and syllable, we determined how well the carbachol (or directed) trial-averaged firing rate function r_{drug} was fit by an additive or multiplicative transformation of the baseline (or undirected) firing rate function r_{base}. The additive model is defined by $r_{drug} = r_{base} + b$; the multiplicative model is defined by $r_{drug} = a \cdot r_{base}$. The best fitting models were found by least squares (i.e, by calculating the value of a or b that minimizes the sum of squared differences between the model and r_{drug}). To evaluate how well each model explained the transformation produced by carbachol (or directed song), we defined a

27

relative distance index calculated as 1 - ($d_{fit,drug}$ / $d_{base,drug}$), where $d_{fit,drug}$ denotes the

Euclidean distance between the best-fit firing rate function and $\mathbf{r_{drug}}$, with $d_{base,drug}$ defined

analogously. This index ranges from zero to one, and quantifies how far the best-fit model

is from $\mathbf{r_{drug}}$, relative to the distance between $\mathbf{r_{base}}$ and $\mathbf{r_{drug}}$. A value of one indicates that the

model fully accounts for the change in firing rate, fitting $\mathbf{r_{drug}}$ perfectly, while a value of zero

indicates that none of the change in firing rate has been accounted for.

Localization of microdialysis probes and recording electrodes

We collected post-mortem histology at the conclusion of experiments to confirm the placement

of microdialysis probes and recording electrodes. HVC was visualized by fluorescent staining for

Parvalbumin (Swant, code 235, monoclonal ab raised in mice, 1:10000), while LMAN was

visualized by fluorescent staining for calcitonin gene-related peptide (Sigma-Aldrich, Cat#

C8198, polyclonal ab raised in rabbits, 1:5000 to 1:10000). The location of microdialysis probes

was indicated by tissue damage within or adjacent to HVC or LMAN. Placement of recording

electrodes was confirmed by tracks left by the electrodes and/or small electrolytic marker

lesions. Dialysis probe placement could not be confirmed bilaterally in a small number of

animals (HVC + LMAN: n = 2/4; HVC only: n = 2/15).
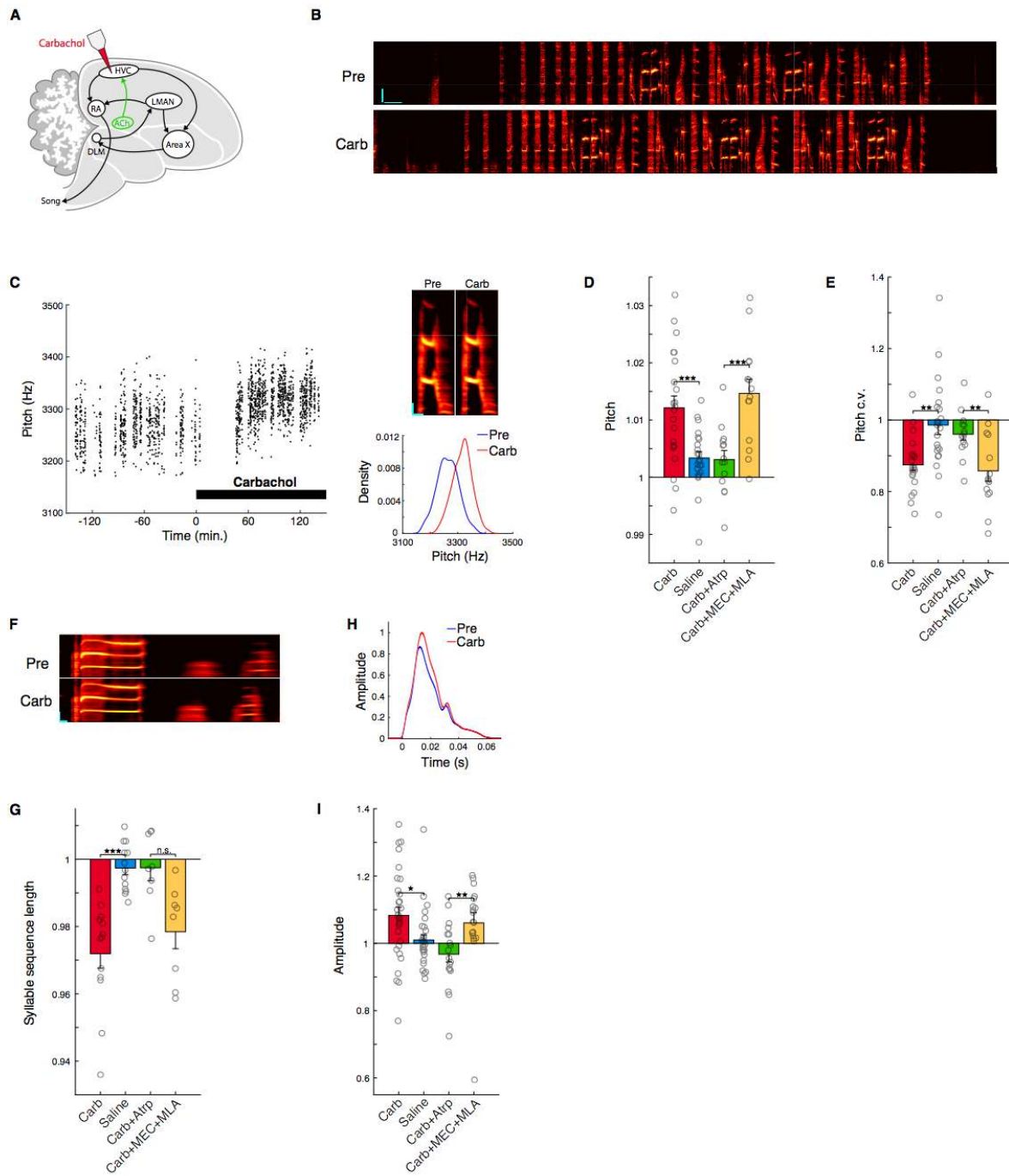
2.8. Figures

Figure 2.1. Activation of muscarinic receptors in HVC increases motor vigor and reduces behavioral variability.

(A) Experiment schematic and song system. HVC receives a cholinergic projection from a basal forebrain homolog (ACh, green).

(B) Example song bouts before and after carbachol (vertical scale bar: 2000Hz, horizontal: 200ms).

(C) Left, time course of raw pitch values for example experiment; top right, average spectrograms for experiment at left before and after carbachol (vertical scale bar: 1000Hz, horizontal: 25ms); lower right, kernel density estimates of pitch distributions for experiment at left before and after carbachol. For panels D, E, G, and I, each point represents one syllable or syllable sequence averaged over experiments.

(D) Normalized (carbachol/baseline) pitch. (Carb vs. Saline, two-tailed sign-rank test, p = 0.00088, n = 22 syllables, 8 birds; Carb+Atrp vs. Carb+MEC+MLA, two-tailed sign-rank test, p = 0.00024, n = 14 syllables, 5 birds).

(E) Normalized (carbachol/baseline) pitch c.v. (Carb vs. Saline, two-tailed sign-rank test, p = 0.0014, n = 22 syllables, 8 birds; Carb+Atrp vs. Carb+MEC+MLA, two-tailed sign-rank test, p = 0.0023, n = 14 syllables, 5 birds).

(F) Trial-averaged spectrograms of a syllable sequence before and after carbachol. Horizontal scale bar: 25ms; vertical scale bar: 2000Hz.

(G) Normalized (carbachol/baseline) syllable sequence length (Carb vs. Saline, two-tailed sign-rank test, p = 0.00024, n = 13 syllable sequences, 8 birds; Carb+Atrp vs. Carb+MEC+MLA, two-tailed sign-rank test, p = 0.078, n = 8 syllable sequences, 5 birds).

(H) Mean +/- s.e.m. amplitude envelopes for one example syllable before and after carbachol. Amplitude envelopes were normalized to the maximum value in the carbachol condition.

(I) Normalized (carbachol/baseline) amplitude. (Carb vs. Saline, two-tailed sign-rank test, p = 0.0117, n = 30 syllables, 8 birds; Carb+Atrp vs. Carb+MEC+MLA, two-tailed sign-rank test, p = 0.0033, n = 18 syllables, 5 birds). *** p < 0.001, ** p < 0.01, * p < 0.05, n.s., not significant.
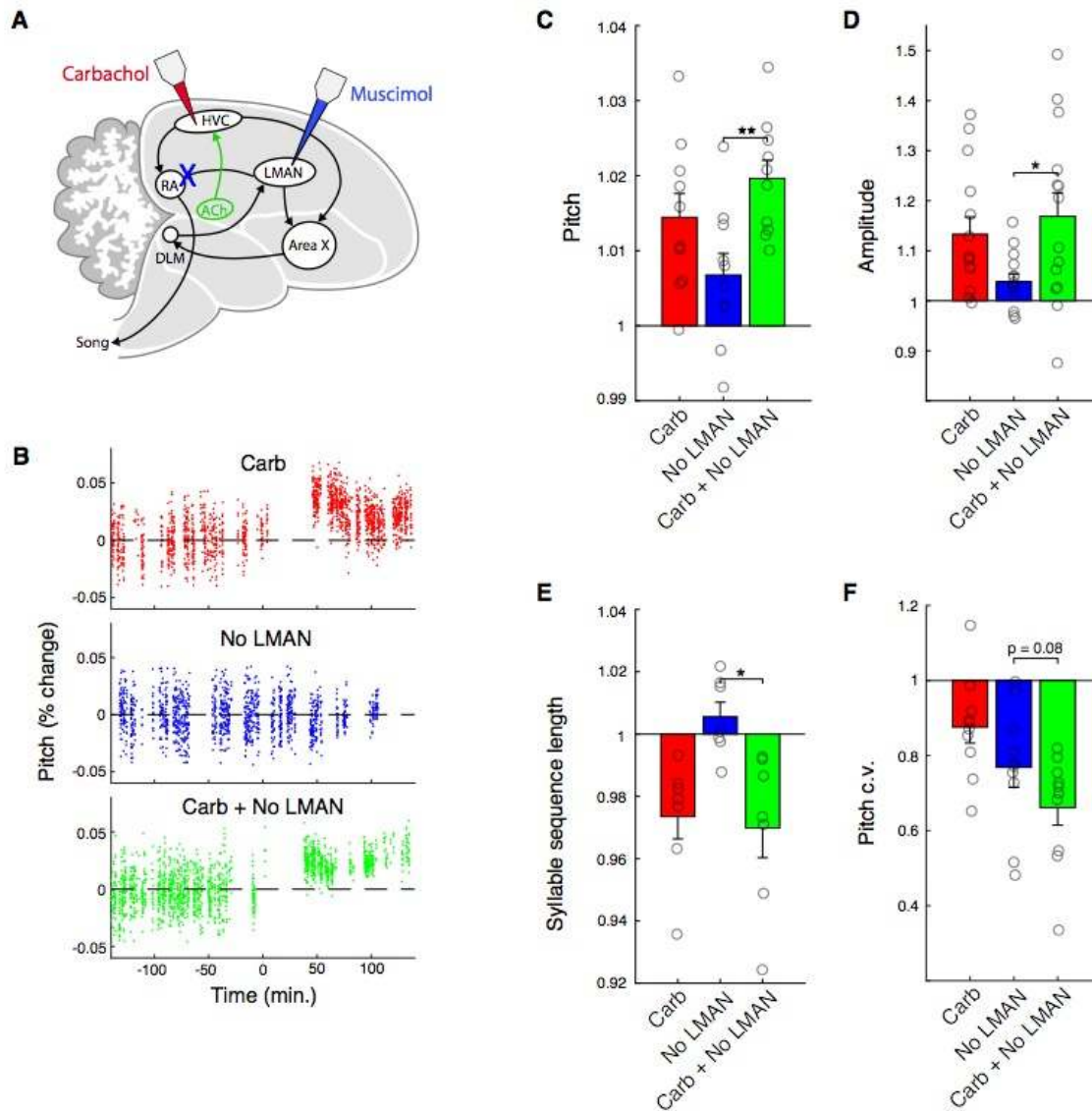
Figure 2.2. Acetylcholine invigorates song via the motor pathway.
(A) Experiment schematic.
(B) Time course of raw pitch values for representative experiments (same syllable). Pitch is plotted as percent change relative to the baseline window for each experiment. For panels C-F, each point represents one syllable or syllable sequence averaged over experiments.
(C) Normalized (drug/baseline) pitch. (n = 10 syllables, 4 birds. Carb+No LMAN vs. No LMAN, two-tailed sign-rank test, p = 0.0020).
(D) Normalized (drug/baseline) amplitude. (n = 14 syllables, 4 birds. Carb+No LMAN vs. No LMAN, two-tailed sign-rank test, p = 0.035).
(E) Normalized (drug/baseline) syllable sequence length. (n = 7 syllable sequences, 4 birds. Carb+No LMAN vs. No LMAN, two-tailed sign-rank test, p = 0.031).
(F) Normalized (drug/baseline) pitch c.v. (n = 10 syllables, 4 birds. Carb+No LMAN vs. No LMAN, two-tailed sign-rank test, p = 0.084). ** p < 0.01, * p < 0.05.
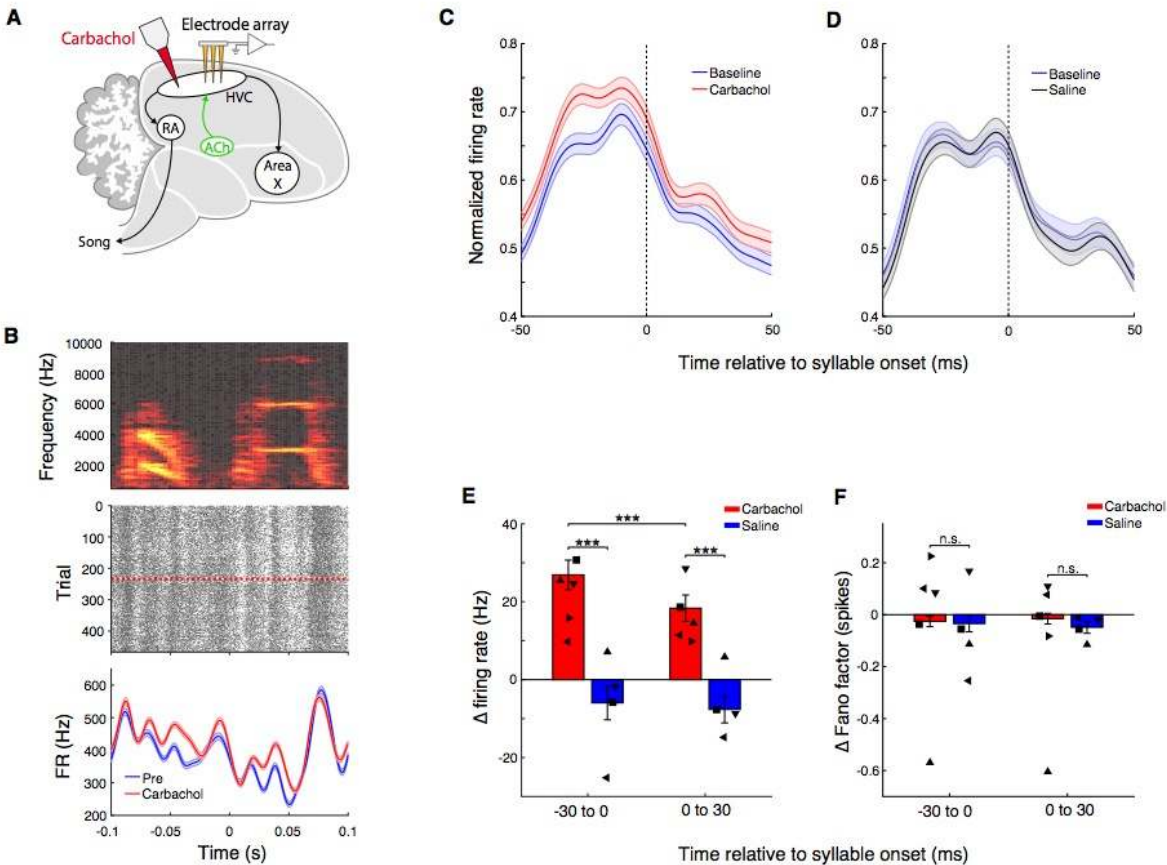
Figure 2.3. Carbachol increases HVC multi-unit firing rates.
(A) Experiment schematic. Carbachol was microdialyzed into HVC while recording neural activity with multi-electrode arrays.
(B) Example multi-unit site aligned to a syllable onset. Top, song spectrogram of the syllable used for alignment. Middle, raster plot of the multi-unit site (red-dashed line = onset of carbachol. Bottom, trial-averaged firing rates before and after carbachol (firing rates smoothed with a 5ms gaussian).
(C) Population-average firing rates aligned to syllable onsets, before and after carbachol. Prior to averaging across sites/syllables, mean firing rates from both before and after carbachol were normalized by the maximum of both conditions in a 100ms window centered on the syllable onset. n = 202 multi-unit sites x syllables, 26 unique multi-unit sites, 5 birds.
(D) Population-average firing rates aligned to syllable onsets, before and after saline, normalized as in panel C. n = 110 multi-unit sites x syllables, 14 unique multi-unit sites, 4 birds.
(E) Change in firing rate after switch carbachol relative to baseline, or after switch to saline relative to baseline. (carb vs. saline in -30 to 0ms window, p = 8.3e-6, rank-sum test; carb vs. saline in 0 to 30ms window, p = 3.1e-4, rank-sum test; carb in -30 to 0ms window vs. carb in 0 to 30ms window, p = 1.1e-4, sign-rank test).
(F) Change in Fano factor after switch to carbachol relative to baseline, or after switch to saline relative to baseline. (carb vs. saline in -30 to 0ms window, p = 0.92, rank-sum test; carb vs. saline in 0 to 30ms window, p = 0.15, rank-sum test). For E and F, markers denote bird averages, bars denote population mean ± s.e.m. *** p < 0.001, n.s., not significant.
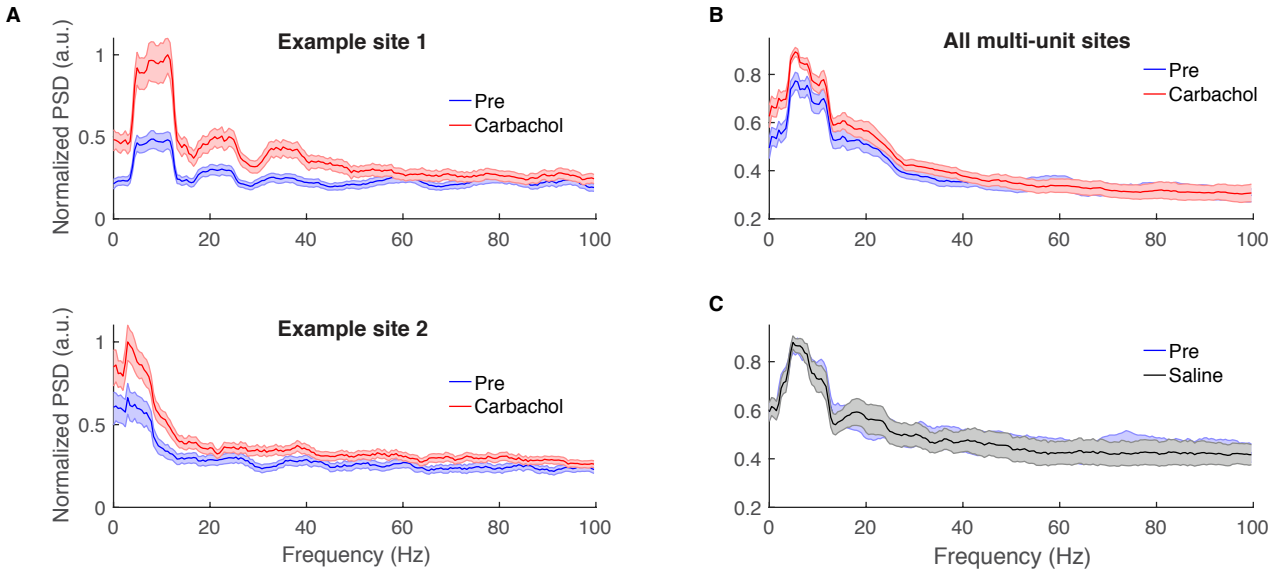
Figure 2.4. Carbachol enhances low-frequency spiking activity in HVC.
(A) Normalized spike train PSDs for two example multi-unit sites from two different birds, before and after microdialysis of carbachol. Error bars denote jackknife 95% confidence intervals.
(B) Population average spike train PSD for all multi-unit sites, before and after switch to carbachol. Each multi-unit site was normalized independently prior to averaging. Error bars denote s.e.m. (n = 25 multi-unit sites from five birds).
(C) Population average spike train PSD for all multi-unit sites, before and after switch to saline, computed as for panel B (n = 12 multi-unit sites from four birds).
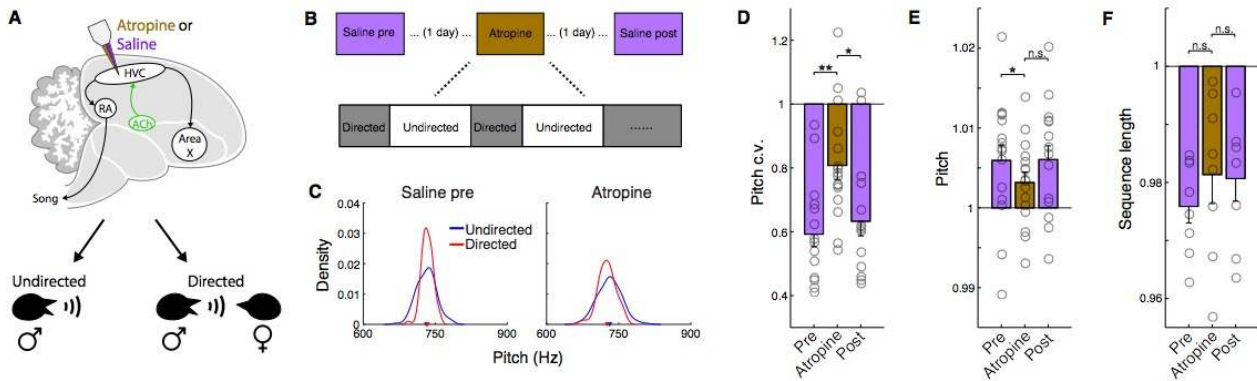
Figure 2.5. Atropine attenuates social modulation of spectral but not temporal features of song.

(A) Experiment schematic.

(B) Directed song was collected on 3 separate days for each bird in the following order: saline/pre, atropine, saline/post, with one day between sessions. See methods for details.

(C) Pitch distributions for one example syllable.

(D) Normalized pitch c.v. (directed/undirected). The reduction in pitch c.v. was significantly attenuated by atropine (pre saline vs. atropine, two-tailed sign-rank test, $p = 0.0028$; post saline vs. atropine, two-tailed sign-rank test, $p = 0.012$).

(E) Normalized pitch (directed/undirected). The increase in pitch was significantly attenuated by atropine compared to the saline pre condition (pre saline vs atropine, two-tailed sign-rank test, $p = 0.046$; post saline vs. atropine, two-tailed sign-rank test, $p = 0.078$). For pitch and pitch c.v., n = 6 birds, 16 syllables.

(F) Tempo measured by normalized sequence length (directed/undirected). The increase in song tempo was not significantly attenuated by atropine (pre saline vs. atropine, two-tailed sign-rank test, $p = 0.20$; post saline vs. atropine, two-tailed sign-rank test, $p = 0.95$). n = 7 birds, 8 syllable sequences. ** $p < 0.01$, * $p < 0.05$, n.s., not significant.
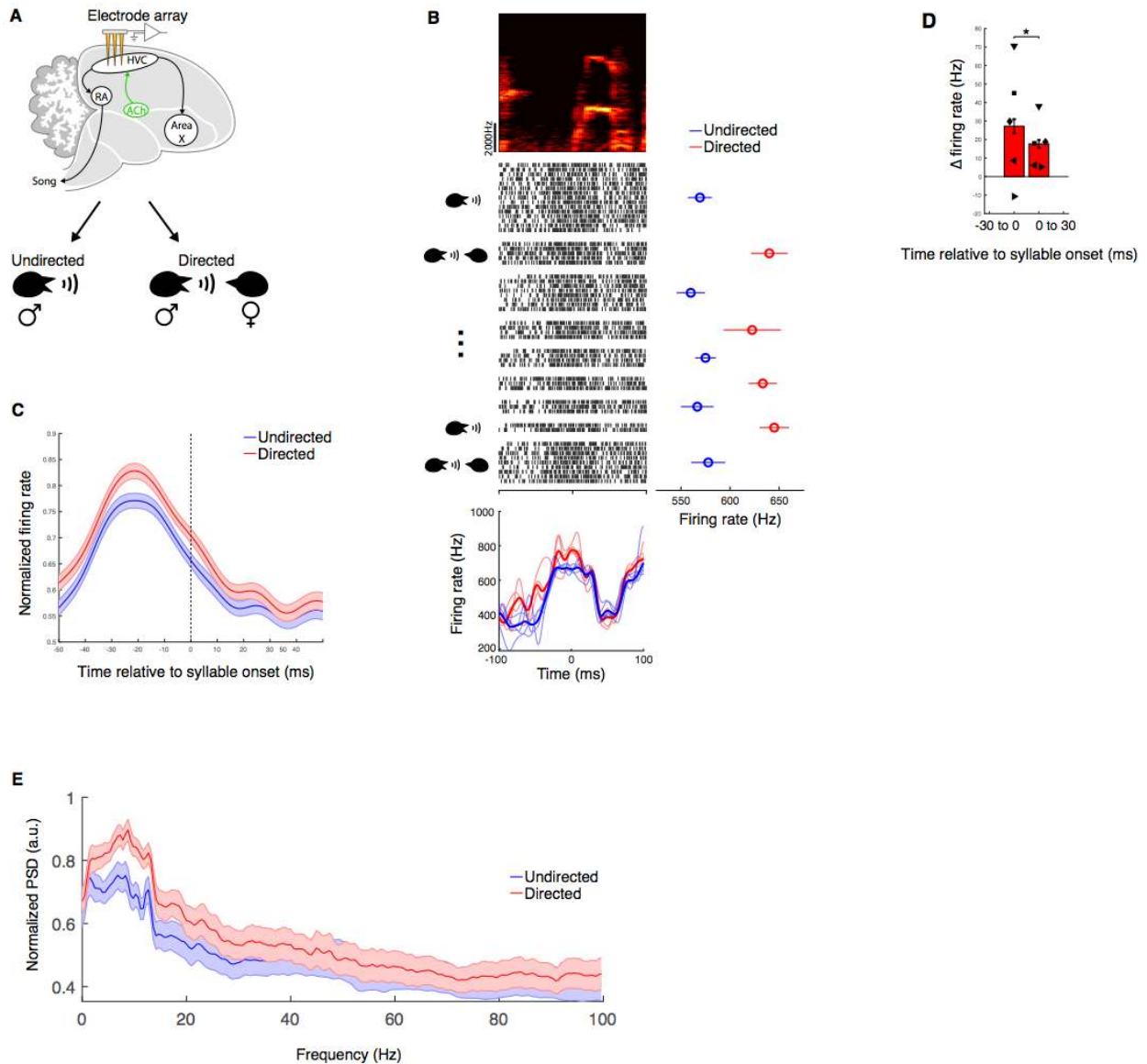
Figure 2.6. HVC activity is modulated by social context.
(A) Experiment schematic. Multi-unit activity in HVC was recorded during interleaved directed and undirected song.
(B) Example multi-unit site aligned to a syllable onset. Top left, spectrogram of song syllable used for alignment. Middle left, raster of the multi-unit site recorded during directed and undirected song on interleaved trials. Trials are plotted chronologically from top to bottom. Spaces separate blocks of directed or undirected trials. Middle right, mean ± s.e.m. firing rates for each block of trials. Firing rates were computed in a 100ms window centered on the syllable onset. Bottom, average smoothed firing rates for this site (firing rates smoothed with a 5ms gaussian). Bold lines show mean firing rates for all trials, light lines show mean firing rates for each block of trials.
(C) Population-average firing rates aligned to syllable onsets, for directed and undirected trials. Prior to averaging across sites/syllables, mean firing rates from directed and undirected trials

were normalized by the maximum of both conditions in a 100ms window centered on the syllable onset. n = 151 multi-unit sites x syllables, 15 unique multi-unit sites, 5 birds.

(D) Change in firing rate on directed trials relative to undirected trials (directed vs. undirected in -30 to 0ms window, $p < 1e-9$, sign-rank test; directed vs. undirected in 0 to 30ms window, $p < 1e-12$, sign-rank test; directed in -30 to 0ms window vs. directed in 0 to 30ms window, $p = 0.011$, sign-rank test).

(E) Population average spike train PSDs for all multi-unit sites, for directed and undirected trials. Each multi-unit site was normalized independently prior to averaging. Error bars denote s.e.m. (n = 13 multi-unit sites from five birds). *** $p < 0.001$, * $p < 0.05$.
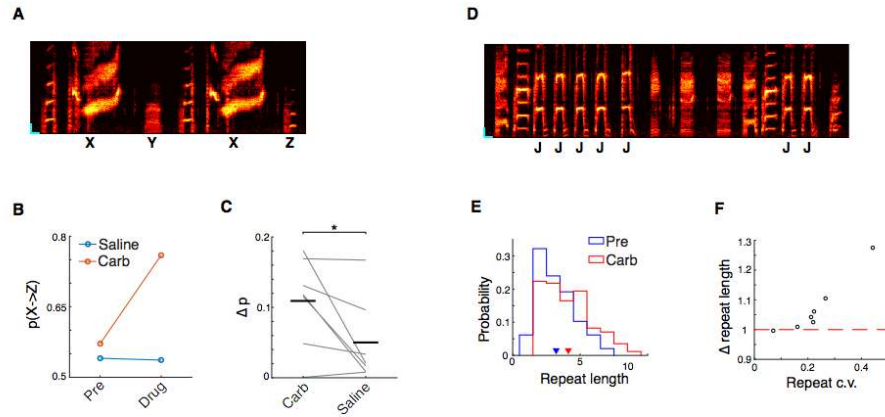
Figure S2.1. Microdialysis of carbachol into HVC alters song sequencing. Related to Figure 2.1.

(A) Spectrogram of a song with a divergent branch point. Syllable 'X' can transition to syllable 'Y' or syllable 'Z'. Horizontal scale bar: 50ms; vertical scale bar: 1000Hz.

(B) Transition probabilities before or after either carbachol or saline for the branch point shown in panel A.

(C) Change in transition probability (see Methods), averaged across all branch points for each bird (carbachol vs. saline, p = 0.047, two-sided sign-rank test, n = 7 birds).

(D) Song spectrogram depicting a repeat syllable (syllable 'J'; Horizontal scale bar: 50ms; vertical scale bar: 1000Hz).

(E) Histogram of repeat counts before and after carbachol for the repeat syllable shown in panel D.

(F) Scatter plot of repeat length c.v. versus the fold change in repeat count with carbachol (p = 0.0012, test for non-zero Pearson's correlation coefficient; n = 6 birds, 7 repeat syllables). * p < 0.05.
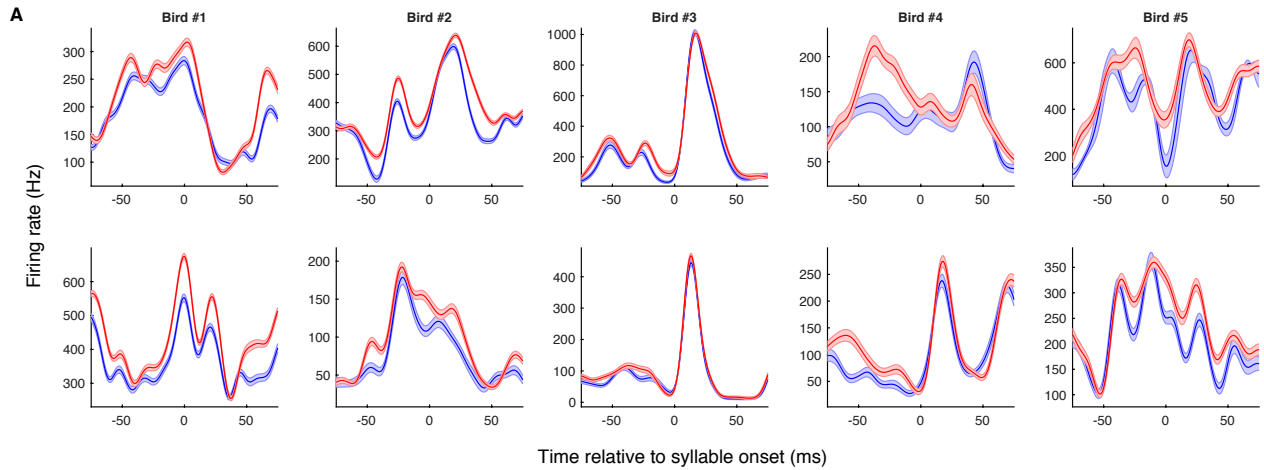
Figure S2.2. Examples of syllable-aligned firing rates before and after carbachol from each bird. Related to Figure 2.3.
 (A) Smoothed firing rates (5ms s.d. gaussian) aligned to syllable-onsets before (blue) and after (red) microdialysis of carbachol into HVC. Two different multi-unit recording sites are shown for each of the five recording birds used in this study.
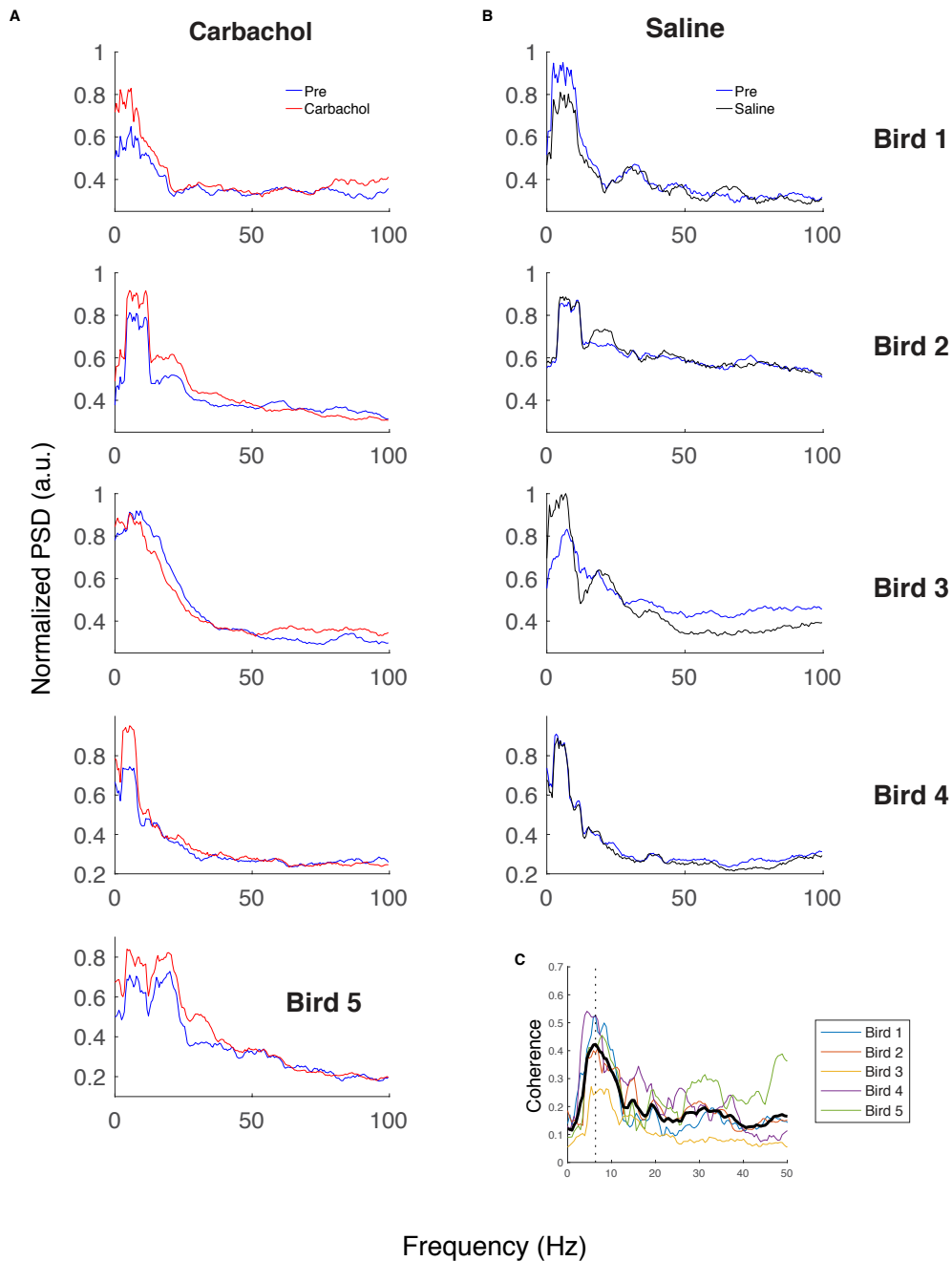
Figure S2.3. Spike train spectra and coherence for individual birds for microdialysis experiments. Related to Figure 2.4.

(A) Bird average spike train PSDs for all multi-unit sites, before and after switch to carbachol. Each multi-unit site was normalized independently prior to averaging.

(B) As for panel A, but for saline control experiments.

(C) Coherence between spike trains and song amplitude for each bird shown in panels A and B. For each bird, we averaged coherence across multi-unit sites from the baseline period of all experiments (black: bird average coherence; dotted line: maximum of bird average coherence at 6.3Hz).
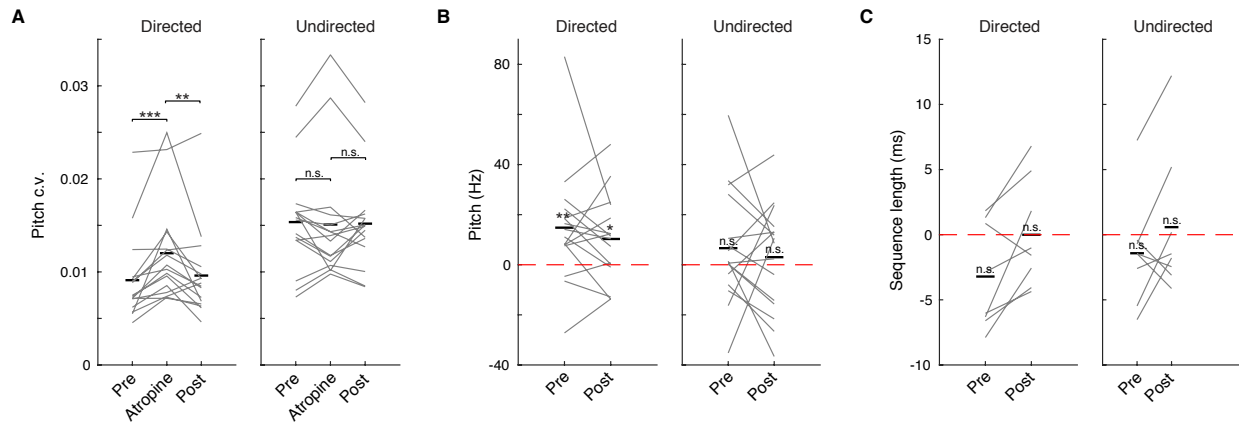
Figure S2.4. Spectral features of directed but not undirected songs are affected by atropine. Related to Figure 2.5.

(A) Raw pitch c.v. values for all syllables for directed (left) and undirected (right) songs. (directed pre vs. directed atropine, p = 0.00024; directed post vs. directed atropine, p = 0.0039; undirected pre vs. undirected atropine, p = 0.34; undirected post vs. undirected atropine, p = 0.41).

(B) Pitch for all syllables. For each syllable, we subtracted its atropine pitch value from both the pre and post saline pitch values in order to reduce the variance within a condition, which is irrelevant. Note also that this transformation does not affect the test statistic used in the sign-rank test. (directed pre vs. directed atropine, p = 0.0045; directed post vs. directed atropine, p = 0.037; undirected pre vs. undirected atropine, p = 0.86; undirected post vs. undirected atropine, p = 0.67). For pitch and pitch c.v., n = 6 birds, 16 syllables

(C) Sequence length for all syllable sequences. For each syllable sequence we subtracted its atropine sequence length value from both pre and post measurements as in panel B. (directed pre vs. directed atropine, p = 0.11; directed post vs. directed atropine, p = 1; undirected pre vs. undirected atropine, p = 0.20; undirected post vs. undirected atropine, p = 0.84). n = 7 birds, 8 syllable sequences. All statistical tests in this figure were performed using the two-sided sign-rank test. ** p < 0.01, * p < 0.05, n.s., not significant.
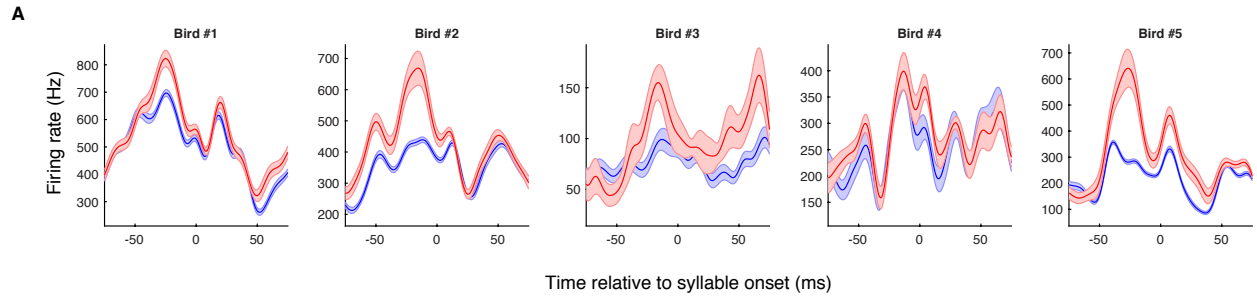
Figure S2.5. Examples of social modulation of HVC firing rates for each bird. Related to Figure 2.6.

(A) Smoothed firing rates (5ms s.d. gaussian) aligned to syllable-onsets for undirected (blue) and directed (red) trials, for one example multi-unit site/syllable from each bird.
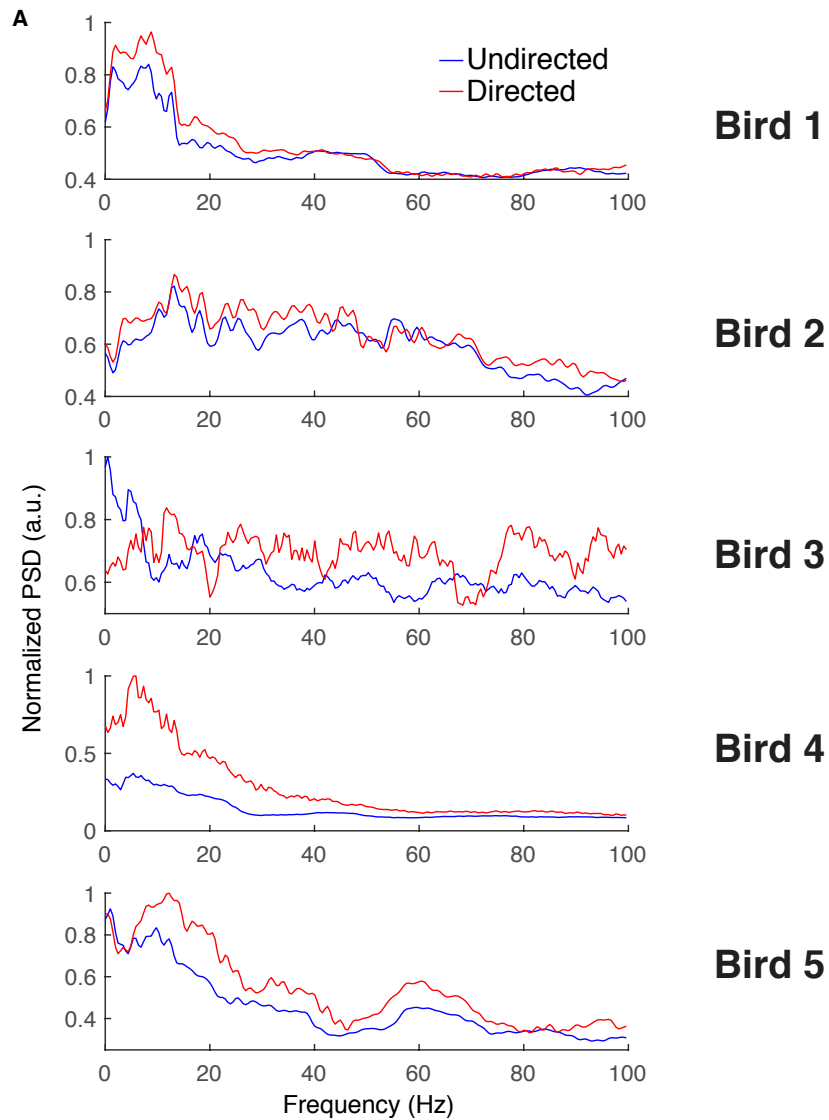
Figure S2.6. Social modulation of spike train spectra for each bird. Related to Figure 2.6. (A) Bird average spike train PSDs for all multi-unit sites, for directed and undirected trials. Each multi-unit site was normalized independently prior to averaging.

Chapter 3: Contributions of the songbird premotor nucleus HVC to acoustic variability

3.1. HVC activity is correlated with acoustic output

Our finding that cholinergic tone in HVC contributes to social modulation of song led us to consider the possibility that acoustic variability observed during undirected song could partly reflect fluctuating levels of acetylcholine in HVC. More generally, we know little about the capacity of trial-by-trial variation in HVC activity to influence behavioral output, regardless of whether or not this involves cholinergic mechanisms. While HVC projection neurons exhibit low trial-to-trial variability in burst timing with respect to acoustic features of song (Hahnloser et al., 2002), it is nonetheless possible that this variability manifests behaviorally, conceivably in the service of trial-and-error learning that underlies song maturation.

To determine the extent to which HVC activity is correlated with acoustic output, we measured trial-by-trial correlations between HVC multi-unit activity and three acoustic features from each syllable—pitch, amplitude, and spectral entropy—to facilitate comparison with a previous study that examined correlations between these features and RA activity (Sober et al., 2008). Firing rates were computed in a 50ms window, offset from the center of the behavioral measurement window by a delay of 30ms to account for the estimated premotor delay between HVC activity and behavioral output (Lynch et al., 2016). One example multi-unit site is shown in Figure 3.1A. For this site, we observed a significant positive correlation between multi-unit activity and pitch (significance assessed by a permutation test, $p < 0.05$). For each behavioral feature, we determined the proportion of significant correlations between the behavioral feature

and HVC activity (Figure 3.1B; n = 5 birds). For pitch and amplitude, we observed that a significant fraction of cases exhibited significant correlations (p = 0.0042 for pitch; p = 1.7e-5 for amplitude; binomial test for significant difference from 0.05; still significant after Bonferroni correction for three comparisons).

In principle, the observed correlations could arise from rapid trial-to-trial fluctuations that are shared between HVC activity and a given behavioral feature. Alternatively, correlations could arise from slower changes to HVC activity and behavior, as might be expected for circadian fluctuations in neuromodulatory tone (though cholinergic neurons in particular are also known to signal phasically over short timescales, see Howe et al., 2017). To determine the timescale over which these correlations are present, we computed correlations between pitch/amplitude and HVC activity offset by a variable lag (in renditions of a given syllable). For pitch, we found that the average magnitude of correlations at lag 0 was similar to that at all other lags examined, suggesting that these correlations arise from processes that covary over long timescales (Figure 3.1C). In contrast, for amplitude we found that the magnitude of correlations peaked at lag 0, suggesting that at least a component of these correlations arise from rapid trial-to-trial fluctuations about the mean (Figure 3.1D). Importantly, neither of these patterns of lagged-correlations precludes the possibility of an underlying causal relationship between HVC activity and the measured acoustic features.

While significant, the magnitude of the correlations we observed for pitch and amplitude was typically low (mean R^2 for pitch: 0.016; for amplitude: 0.025). Weak correlations would result if most of the variability in behavior is not inherited from HVC. Alternatively, activity that is causally related to vocal output for a particular syllable may be better represented in the activity of HVC_{RA} projection neurons, whose activity is most proximal to motor output. To

evaluate this latter possibility, we identified bursts from isolated HVC projection neurons[1] of

Bengalese finches that occurred during or just prior to harmonic stack syllables (n = 13 bursts

from 5 birds). For each burst/syllable pair, we computed the Pearson's correlation coefficient

between spikes per burst and pitch or amplitude (see Methods for details). Isolated HVC

projection neurons exhibited substantially stronger correlations with pitch and amplitude than we

observed in our multi-unit data (mean R^2 for pitch: 0.25; amplitude: 0.35). Histograms of the

correlation coefficients for pitch and amplitude are shown in Figure 3.1E. Thus, HVC projection

neurons exhibit strong correlations with acoustic output, consistent with the notion that HVC

contributes to acoustic variability.

3.2. Greater HVC activity predicts lower behavioral variability

One of the more surprising findings reported in Chapter 2 is that cholinergic tone in HVC

regulates behavioral variability, given that previous studies that have manipulated HVC activity

have not reported reductions in behavioral variability (Hamaguchi et al., 2016; Long and Fee,

2008; Zhang et al., 2017). Trial-by-trial behavioral variability is essential for reinforcement

learning; as such, understanding the neural origins of this variability is of central importance. We

considered a range of possible mechanisms that could explain our finding that microdialysis of

carbachol into HVC reduces pitch variability. To ground discussion, let us consider a simple

model in which pitch (Y) is a weighted sum of contributions of many HVC neurons (X_i), passed

through an arbitrary non-linear function f, i.e. $Y = f(\sum_i w_i X_i)$. A simplified situation in which

---

[1] Note that the projection target of these neurons was not confirmed, i.e. they could project to either RA or Area X (and possibly Avalanche, though these neurons are substantially less abundant). However, both HVC_{RA} and HVC_X neurons are readily identified by their distinctive firing properties, namely bursting activity that is precisely time-locked to specific acoustic elements.

pitch is entirely controlled by two neurons is schematized in Figure S3.1. As shown, changes to the means, variances, and pairwise covariances of HVC neurons all have the capacity to change pitch variance[2]. Acetylcholine has been shown to modulate each of these three statistics, providing additional motivation for the following analyses (Chen et al., 2015; Desai, 2006; Goard and Dan, 2009; Herrero et al., 2008).

As discussed in Chapter 2, we found little evidence to support the possibility that reduced variability in HVC activity is responsible for the reduction in behavioral variability. We also found little evidence to support the possibility that covariance between simultaneously recorded multi-unit sites was significantly affected by carbachol. We measured the covariance in spike counts between simultaneously recorded multi-unit sites in HVC before and after carbachol (spike counts computed in 50ms window prior to syllable onsets). Carbachol did not produce a significant change in spike count covariances (data not shown; normalized covariance = 0.99; two-tailed sign-rank test for baseline vs. carb, $p = 0.32$; n = 815 pairs x syllables in 5 birds).

In contrast, our finding that carbachol increased HVC firing rates lends some support to the possibility that a change to the mean of HVC activity could drive the reduction in pitch variability. One caveat with these analyses is that we are not directly measuring activity of the HVC$_{RA}$ neurons, whose activity is most proximal to behavioral output. However, as we elaborate in the discussion, a number of other observations indicate that carbachol increases the activity of the HVC$_{RA}$ projection neurons, suggesting this as a plausible mechanism for the reduction in pitch variability and the other observed behavioral changes. Increased activity of HVC projection neuron activity could reduce behavioral variability by a saturation-like mechanism, assuming

---

[2] Further insight into the manner in which these three statistics contribute to variance in Y can be gained by treating Y and the X_i as random variables, and approximating the variance in Y as a Taylor series expansion around the mean.

that downstream motor units have saturating input/output relationships (Garst-Orozco et al., 2014), or by suppressing the intrinsic dynamics of the RA network (see Discussion).

We sought additional evidence that the magnitude of HVC projection activity has the capacity to regulate behavioral variability. Specifically, we hypothesized that natural variation in PN activity during undirected song would be systematically associated with behavioral variability, with greater PN activity predicting lower behavioral variability. To address this, we identified bursts from isolated PNs[3] of Bengalese finches that occurred during or just prior to harmonic stack syllables (n = 12 bursts from 5 birds). For each burst, we binned trials by the number of spikes per burst and calculated the pitch c.v. within each bin. Two example bursts are shown in Figure 3.2A. In both of these cases, more spikes per burst is associated with lower pitch variability. To summarize this relationship for each burst, we calculated the mean slope of pitch c.v. versus spikes per burst (Figure 3.2B). Across bursts, the sign of this relationship was significantly less than zero, indicating that greater projection neuron activity is generally associated with lower pitch variability ($p = 0.032$, one-tailed sign-rank test). These data are consistent with the view that greater projection neuron activity drives lower behavioral variability.

3.3. Methods

Experimental procedures for collecting electrophysiological and audio data were conducted as described for the methods section in Chapter 2. The animals used for these analyses comprise a subset of the animals used for the recording experiments presented in Chapter 2. Unless stated otherwise, other relevant methods are consistent with those described in Chapter 2.

---

[3] As for the analyses presented in section 3.1, the projection target of these neurons was not confirmed.

Measuring pitch, amplitude, and spectral entropy

Pitch contours were computed for syllables with well-defined harmonic structure as described in Chapter 2. Amplitude was calculated essentially as described in chapter 2, with minor modifications. Spectral entropy was computed by calculating a normalized PSD for each syllable, then computing $-\sum_i p_i ln(p_i)$, where p_i denotes the normalized power in frequency bin i. For all behavioral features, we excluded measurements using the outlier procedure described in Chapter 2.

Analysis of correlations between multi-unit activity and acoustic features

Multi-unit activity was aligned to syllable onsets and smoothed with a 5ms gaussian kernel. For each trial, the smoothed firing rate was averaged over a 50ms window, offset by a 30ms delay from the center of the window used for measuring a given behavioral feature. Each behavioral feature was averaged over a 20ms window, typically just after the onset of a given syllable. We excluded cases with fewer than 10 trials or mean firing rates less than 50Hz.

Analysis of correlations between projection neuron activity and acoustic features

We analyzed bursts that occurred during a harmonic stack syllable, or that occurred within 50ms of the onset of the harmonic portion of the syllable, measured from the center of the burst. Pitch and amplitude were averaged over a 20ms window. For bursts that occurred during the syllable, the pitch/amplitude window started 30ms after the center of the burst. For bursts that occurred prior to the harmonic portion of the syllable, the pitch window started at the onset of the harmonic portion of the syllable. For measurements of the mean slope between binned spikes per

burst and pitch c.v., bins with fewer than five trials were excluded. For computing correlations

between spikes per burst and pitch or amplitude, we excluded cases with fewer than 10 trials.

3.4. Figures
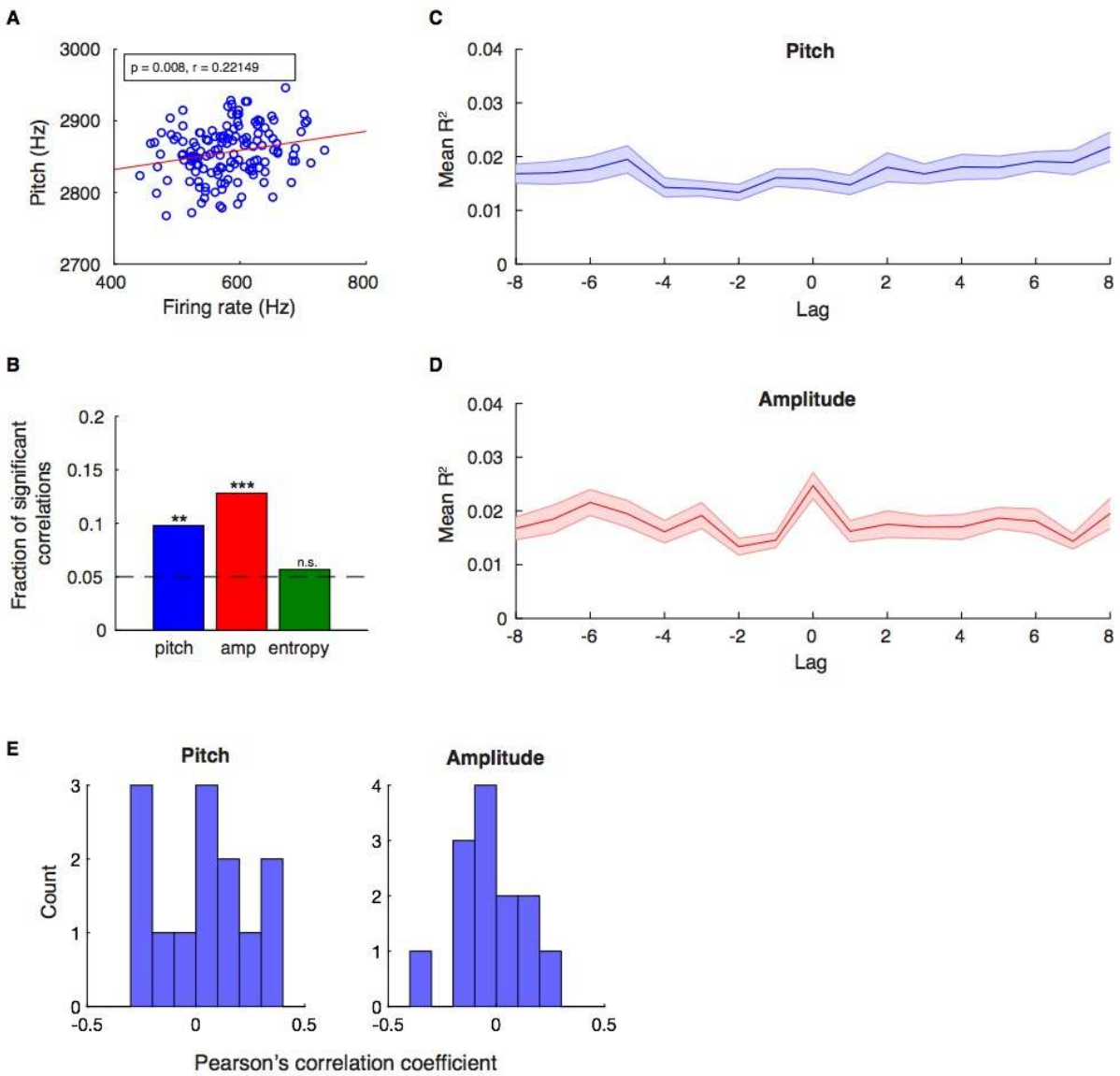
Figure 3.1. HVC activity is correlated with acoustic features.
(A) Example multi-unit exhibiting a significant positive correlation between pitch and firing rate.
Each point is the pitch/firing rate for a given syllable rendition.
(B) Proportion of significant correlations between HVC multi-unit activity and pitch, amplitude,
and spectral entropy. ** $p < 0.01$, *** $p < 0.001$, n.s. not significant.

(C) Mean ± s.e.m. R^2 (coefficient of determination) for pitch/HVC multi-unit firing rate correlations as a function of lag.
(D) As for panel C, for amplitude/firing rate correlations.
(E) Histogram of Pearson's correlation coefficients between HVC projection neuron spikes per burst and pitch (left) or amplitude (right).
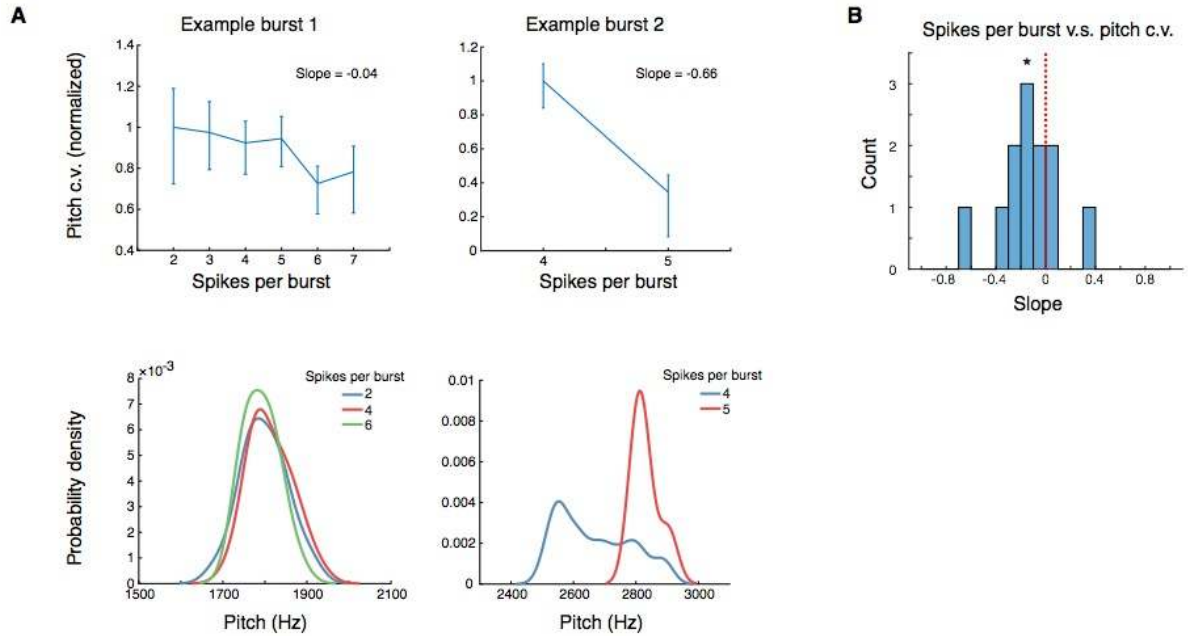
Figure 3.2. Greater HVC projection neuron activity predicts lower behavioral variability.
(A) Two example projection neuron bursts from two different birds. Top, pitch c.v. for a nearby harmonic syllable, computed as a function of spikes per burst. Pitch c.v. values were normalized to the bin with the maximum pitch c.v. Bottom, raw pitch distributions, separated by spikes per burst.
(B) Mean slopes of projection neuron spikes per burst versus pitch c.v., for all bursts. * $p < 0.05$.
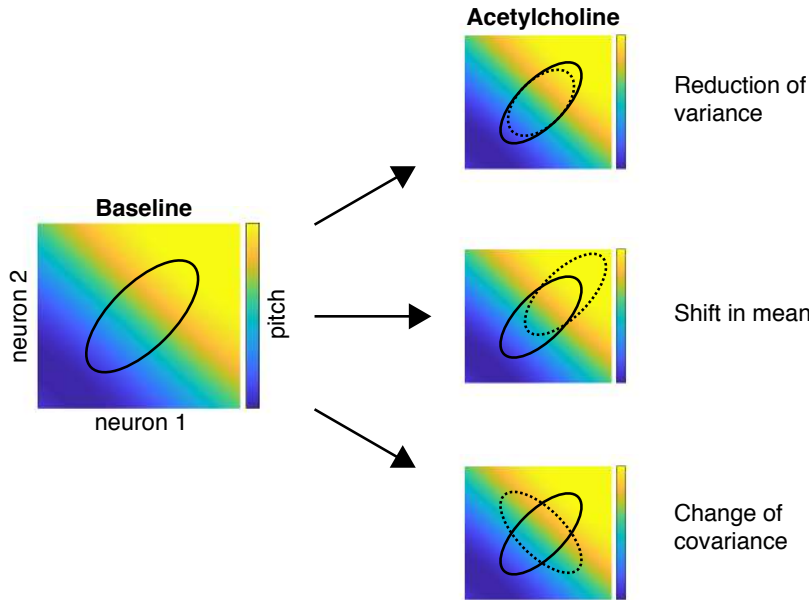
Figure S3.1. Schematic of mechanisms for changing behavioral variability.
Left: We consider a simplified situation in which the activity of two neurons determines pitch. The activity of these neurons is mapped to pitch by the function indicated in the heat map; note that pitch saturates as the activity of these two neurons increases. The black ellipse indicates the covariance of these two neurons; they are positively correlated at baseline.
Right, top: Acetylcholine could reduce pitch variability by reducing the variability of each neuron (dotted ellipse). Right, middle: Variability could be reduced by increasing the mean activity of the two neurons, into the saturating part of the pitch function. Right, bottom: Variability could be reduced by altering the covariance of the two neurons. After acetylcholine, the neurons covary in a way that aligns with an axis of low variability in pitch.

Chapter 4: Discussion

Though motor cortical regions receive extensive projections from cholinergic neurons and other neuromodulatory systems, little is known about how any neuromodulator contributes to motor skill execution by direct action on cortical motor structures (Vitrac and Benoit-Marand, 2017). We examined how the canonical neuromodulator acetylcholine affects motor behavior by direct action on premotor circuitry, motivated by observations that physiological arousal influences both motor behavior and cholinergic signaling. We found that acetylcholine acts directly on motor forebrain circuitry to invigorate movement, increasing the pitch, amplitude, tempo, and stereotypy of song. We further demonstrate that acetylcholine contributes to behavioral changes observed during courtship song, thereby linking acetylcholine to motor invigoration observed during aroused behavioral states. Both modulation of cholinergic tone and courtship song were associated with higher firing rates and enhancement of low-frequency activity in the premotor nucleus HVC, paralleling previous findings in non-motor brain regions that acetylcholine contributes to enhanced activity and low-frequency oscillations observed during active and attentive states (Fu et al., 2014; Gu et al., 2017; Herrero et al., 2008). Finally, by demonstrating that cholinergic enhancement of vigor occurs independently of the songbird basal-ganglia, we identify direct cholinergic action on the descending forebrain motor pathway as a mechanism for the control of motor vigor.

4.1. Neuromodulatory control of motor vigor

Our finding that acetylcholine acts on motor forebrain circuitry to invigorate movement compliments previous studies that have focused on the role of striatal dopamine in the control of motor vigor. A general correlation between dopamine levels and motor vigor is supported by numerous studies in animal models that have either depleted (Panigrahi et al., 2015; Ungerstedt, 1971) or enhanced (da Silva et al., 2018) dopaminergic signaling. In general, dopamine depletion leads to substantial reductions in spontaneous movements and movement velocity. Similarly, in humans, slowed movements (bradykinesia) is a cardinal symptom of the deterioration of the dopaminergic system that occurs during Parkinson's disease (Berardelli et al., 2001). A number of observations indicate that dopamine may be especially important for invigorating motor behavior to obtain reward, i.e., that the modulatory effects of dopamine on motor vigor are primarily motivational in nature (Mazzoni et al., 2007). Rewarding stimuli are well-known to enhance motor vigor: primates and humans saccade and reach more vigorously to target locations paired with reward (Summerside et al., 2018; Takikawa et al., 2002; Xu-Wilson et al., 2009). Supporting the hypothesis that reward invigorates movement via dopaminergic mechanisms, patients with Parkinson's disease are less sensitive to modulation of motor vigor by reward (Manohar et al., 2015). Conversely, pharmacological enhancement of dopaminergic signaling increases the effect of reward on motor vigor (Beierholm et al., 2013; Wardle et al., 2011).

Notably, however, invigoration of movement can occur under general states of arousal, even when reward is not explicitly manipulated or available. Striking examples of this link between arousal and movement invigoration include anecdotal reports of extraordinary feats of "hysterical strength" in life-or-death situations, such as lifting a car to free an entrapped victim.

Corroborating these anecdotal accounts, studies conducted in humans have documented that unexpected auditory stimuli facilitate eye movements (DiGirolamo et al., 2016) and reduce motor response time in task settings (Bertelson, 1967; Nebes and Brady, 1993). Similarly, stimulating music can speed reaction time and increase grip strength (Bishop et al., 2009; Karageorghis et al., 1996), and viewing unpleasant images can increase step size during gait initiation (Bouman et al., 2015). These studies are complemented by findings in animal systems that physiological measures of arousal, such as pupil diameter and heart rate, are correlated with faster reaction time in behavioral tasks (Lovett-Barron et al., 2017; McGinley et al., 2015). While previous studies have primarily focused on the role of dopamine in movement invigoration, a number of observations from human and animal studies suggest that this arousal-mediated enhancement of motor vigor can occur independently of dopaminergic mechanisms. Patients with Parkinson's disease can exhibit 'paradoxical' movement in situations that provoke extreme emotion (Bonanni et al., 2010; Glickstein and Stein, 1991), and rats with dopaminergic lesions induced by 6-OHDA, can swim effectively when placed in cold water (Marshall et al., 1976). Broadly, the relationship between arousal and motor vigor, rather than the expectation of reward per se, suggests that a broader recruitment of neuromodulatory brain regions may contribute to motor invigoration.

Acetylcholine in particular has strong associations with physiological arousal (Lee and Dan, 2012). Acetylcholine contributes to widespread changes in neural activity that occur during transitions in behavioral state (Buzsaki et al., 1988; Metherate et al., 1992), and the activity of cholinergic neurons is correlated with arousal as measured by pupil diameter (Reimer et al., 2016). Further, cholinergic neurons in the basal forebrain are activated by both positive and negative stimuli (Hangya et al., 2015), suggesting that cholinergic neurons may contribute to

modulation of motor vigor by salient stimuli, irrespective of valence. Linking acetylcholine to

motor behavior, a number of studies have reported that cholinergic neurons become more active

during locomotion, whisking, and other non-locomotor movements (Eggermann et al., 2014;

Hangya et al., 2015; Nelson and Mooney, 2016; Reimer et al., 2016). Our finding that a

component of motor invigoration observed during courtship song is subserved by central action

of cholinergic systems directly demonstrates that acetylcholine contributes to motor invigoration

under heightened states of arousal.

Conversely, we suggest that some movement disorders that include decreased speed,

force, and stereotypy of movements, may reflect in part disrupted cholinergic signaling in

premotor centers. Particularly noteworthy in this respect is the slowing of gait, reduced force

generation, and loss of verbal fluency that are frequently observed in patients with Alzheimer's

disease (Buchman et al., 2007; Ferris and Farlow, 2013; Goldman et al., 1999), which is

principally associated with the loss of cholinergic neurons in the basal forebrain and diminished

cholinergic innervation of the cortex (Francis et al., 1999). Indeed, loss of movement vigor may

precede, and be predictive of, subsequent cognitive decline in Alzheimer's and other diseases

(Buchman et al., 2007). An underappreciated role of cortical cholinergic signaling in the

invigoration of movements, as indicated by our findings, may both explain this link, and account

for some of the ameliorative effects on movements of pro-cholinergic treatments (Ferris and

Farlow, 2013).

4.2. Neuromodulatory contributions to social modulation of song

It is important to note that multiple neuromodulatory systems may be engaged simultaneously to influence vigor, a point made especially apparent by social modulation of song. Previous studies in songbirds have implicated dopaminergic and noradrenergic signaling in the social modulation of song (Glaze et al., 2017; Leblois et al., 2010), complementing our finding that acetylcholine contributes to social modulation of song via the premotor nucleus HVC. Indeed, the absence of a complete block of social modulation by atropine suggests that multiple neuromodulators and loci of action contribute to social modulation of song, (Glaze et al., 2017; Leblois et al., 2010). The multiplicity of neuromodulatory systems apparently engaged during courtship song parallels the general observation that multiple neuromodulators contribute to global changes in brain activity that accompany transitions in behavioral state, e.g. the transition from sleep to wakefulness (Lee and Dan, 2012). Consistent with the notion that multiple neuromodulators act in a cooperative manner to regulate behavioral state, a recent study found that the activity of a number of neuromodulatory cell groups are correlated with physiological measures of arousal in both zebrafish and mice (Lovett-Barron et al., 2017). Thus, while our findings reveal an important role for acetylcholine in the social modulation of song, it is likely that the totality of behavioral changes observed during courtship song reflect the coordinated action of multiple neuromodulators acting simultaneously in different brain regions.

4.3. Neural mechanisms underlying cholinergic invigoration of song

How does acetylcholine affect the activity of the different cell classes within HVC? A number of observations from our data and previous studies suggest that acetylcholine increases the activity of the HVC_{RA} projection neurons *in vivo*, an effect that is likely to account for the behavioral changes produced by microdialysis of carbachol into HVC. First, we found that removing the contribution of the songbird basal-ganglia to song by inactivation of LMAN does not prevent the increase in pitch, amplitude, or tempo produced by carbachol, which indicates that, at a minimum, acetylcholine affects the activity of HVC_{RA} projection neurons. Second, agonists of muscarinic acetylcholine receptors depolarize HVC projection neurons (both HVC_{RA} and HVC_X) and hyperpolarize HVC interneurons *in vitro* (Shea et al., 2010), which is likely to translate to an excitatory influence on HVC_{RA} neurons *in vivo*. Finally, we found that acetylcholine increases multi-unit firing rates in HVC in singing birds, an observation which suggests that acetylcholine increases the activity of one or both major cell classes in HVC.

How does increased activity of HVC_{RA} neurons translate into increased motor vigor? Within HVC, enhanced excitability of HVC_{RA} neurons is expected to speed the propagation of activity through synaptically coupled pools of projection neurons that are hypothesized to underlie song production (Long and Fee, 2008), thereby increasing the tempo of song. Downstream of HVC, a number of observations indicate that greater activity of HVC_{RA} neurons would increase the activity of RA projection neurons, ultimately driving increased pitch and amplitude. Neurophysiological evidence for this model is furnished by the observation that injections of carbachol into HVC of anaesthetized songbirds increase spontaneous activity within RA (Shea and Margoliash, 2003). Behaviorally, pharmacological reduction of inhibition onto RA projections neurons increases pitch and amplitude (Miller et al., 2017), suggesting that

microdialysis of carbachol into HVC has a similar excitatory influence on RA projection neurons. Downstream of RA, anatomical and functional evidence indicates that increased activity of RA projection neurons may increase pitch via an excitatory influence on particular syringeal muscles (Sober et al., 2008): pitch is positively correlated with syringeal muscle activation in some songbird species (Goller and Riede, 2013), and stimulation of syringeal muscles drives increased pitch in Bengalese finches (Srivastava et al., 2015).

More broadly, a model in which cholinergic excitation of motor cortex drives increased motor vigor is consistent with a number of observations in other systems. Acetylcholine increases the excitability of pyramidal neurons in layer 5 of rat primary motor cortex (Desai, 2006), which may facilitate increased force production via activation of downstream motorneurons (Cheney and Fetz, 1980; Evarts, 1968). This idea is supported by the observation that nucleus basalis stimulation increases the amplitude of vibrissae movements caused by electrical stimulation of motor cortex, an effect that is blocked by local cortical application of the muscarinic antagonist atropine (Berg et al., 2005). Cholinergic excitation of motor cortex may also underlie observations from human fMRI studies that have found a positive correlation between activation of motor cortex and force production (Dai et al., 2001; Spraker et al., 2007). Beyond altering movement force, computational studies have demonstrated that neuromodulators can scale the speed of motor outputs by altering the gain of motor cortical neurons (Stroud et al., 2018), suggesting an expansive capacity of acetylcholine and other neuromodulators to alter the vigor of multiple movement parameters.

4.4. Contributions of HVC to acoustic variability

Trial-by-trial variability in behavioral output is essential for reinforcement learning, providing a substrate by which organisms adapt their behavior in complex environments. For these reasons, a large body of work in both songbirds and mammals has aimed to determine how the brain generates and regulates behavioral variability. Our results add to this discussion and suggest novel mechanisms by which the brain controls variability.

In the context of song control, our finding that acetylcholine can operate on HVC to reduce behavioral variability is somewhat surprising. Previous studies that have manipulated HVC activity have not reported a reduction in behavioral variability (Hamaguchi et al., 2016; Long and Fee, 2008; Zhang et al., 2017). In contrast, lesions and pharmacological inactivation of the AFP output nucleus LMAN reduce pitch variability substantially (Hampton et al., 2009; Kao et al., 2005; Stepanek and Doupe, 2010). The observation that HVC projection neurons exhibit extremely low trial-to-trial variability has further contributed to the impression that HVC does not introduce substantial behavioral variability (Hahnloser et al., 2002).

Mechanistically, the observation that increasing cholinergic signaling in HVC drives a reduction in behavioral variability could be explained in a number of ways (Figure S3.1). Perhaps the simplest possible explanation is that acetylcholine reduces neural variability in HVC. As carbachol had no effect on the Fano factor, and either increased or did not affect spike count variance, we found little evidence to support this possibility. Alternatively, acetylcholine could reduce behavioral variability by altering the correlation structure of HVC activity (e.g., Kaufman et al., 2014). While we did not find evidence that carbachol altered the correlation structure of HVC activity, as assessed by measuring changes to the spike count covariance of simultaneously recorded multi-unit sites, addressing this possibility definitively would require estimating the full

mapping between HVC population activity and behavioral output. Finally, carbachol could reduce behavioral variability through a saturation-like mechanism by altering the magnitude of input to RA. Though we were unable to directly determine how carbachol affects the activity of HVC projection neurons, a number of observations suggest that carbachol increases the activity of HVC_{RA} projection neurons, as discussed in the preceding discussion section. Further, our observation that greater HVC projection neuron activity predicts lower behavioral variability during undirected song lends direct support to this possibility.

Such a mechanism could operate at the level of single neurons in RA: altered drive to RA could push RA projection neurons to the saturating part of their response functions, a mechanism that has been proposed to partly account for the developmental reduction in vocal variability (Garst-Orozco et al., 2014). Alternatively, network-level dynamics within RA may be critical for understanding the reduction in variability. One potential issue with single-cell models is that it is unclear if RA neurons operate near the saturating part of their response functions. Additionally, due to the convergence of a large number of RA projection neurons onto a few motor effectors, changes to correlated variability across the population of RA neurons are expected to substantially impact behavioral variability (Darshan et al., 2017). This directly motivates consideration of network-level mechanisms.

In sensory cortices, it is well-documented that stimuli suppress both individual and correlated neural variability, effects that are thought to arise from intrinsic cortical dynamics (Churchland et al., 2010). A variety of network models with different dynamical behavior have been proposed to account for this effect (Deco and Hugues, 2012; Hennequin et al., 2018). One relevant phenomenon is that increasing the strength of input to a network tends to suppress its intrinsic dynamics (Mastrogiuseppe and Ostojic, 2018; Rajan et al., 2010). We suggest that

acetylcholine reduces behavioral variability via a similar mechanism. In this model, external perturbations to RA—originating from LMAN, for example—are amplified by the dynamics of the RA network and drive increased correlations between RA projection neurons. Stronger input to RA driven by higher cholinergic tone in HVC suppresses these intrinsic dynamics, reducing correlations within RA, and ultimately reducing behavioral variability. Within RA, the extensive recurrent inhibition is likely to be critical for shaping its dynamical behavior and altering correlations between the RA projection neurons (Miller et al., 2017).

This model makes a number of experimentally testable predictions. First, increasing the strength of input to RA from HVC should reduce the behavioral effect of perturbations introduced by LMAN, as generated by electrical microstimulation within LMAN, for example (Kao et al., 2005). Second, increased drive to RA should decorrelate RA projection neurons. By combining population-level recordings of RA with manipulations of HVC and LMAN, future studies may test these hypotheses, and clarify the mechanisms underlying central contributions to acoustic variability.

4.5. Parallels between cholinergic modulation of motor and other brain regions

Our findings also suggest parallels between the manner in which acetylcholine modulates motor and other brain regions. Broadly, acetylcholine has a well-established role in mediating widespread changes to brain activity observed in states of heightened arousal (Buzsaki et al., 1988; Metherate et al., 1992), in general agreement with our observation that acetylcholine contributes to behavioral changes observed during courtship song—a highly aroused behavior state—via action on motor forebrain regions. The specific changes we observed to HVC activity

following dialysis of carbachol are also consistent with observations in other systems. We observed increased activity in HVC following local application of the cholinergic agonist carbachol, in general agreement with the excitatory effects of acetylcholine often observed in sensory brain regions (Thiele, 2013). In particular, acetylcholine has been shown to underlie increases in stimulus-driven activity that occur during more vigilant behavioral states, such as selective attention and locomotion (Fu et al., 2014; Herrero et al., 2008). Our finding that carbachol enhances low-frequency activity in HVC (below 10Hz) also bears some resemblance to observations that acetylcholine contributes to theta oscillations (2-10Hz) in the hippocampus (Gu et al., 2017; Vandecasteele et al., 2014). Paralleling our findings and those in sensory systems, acetylcholine has been shown to contribute to increased theta power observed during active behavioral states (Gu et al., 2017). Future studies may aim to determine the extent to which these apparent commonalities arise from conserved neural connectivity and dynamical behavior operating on a more fundamental level, e.g. specific connectivity motifs between defined neural cell-types (Chen et al., 2015).

References

Asogwa, N.C., Mori, C., Sánchez-Valpuesta, M., Hayase, S., and Wada, K. (2018). Inter- and intra-specific differences in muscarinic acetylcholine receptor expression in the neural pathways for vocal learning in songbirds. J. Comp. Neurol. *526*, 2856–2869.

Ball, G.F., Nock, B., Wingfield, J.C., McEwen, B.S., and Balthazart, J. (1990). Muscarinic cholinergic receptors in the songbird and quail brain: A quantitative autoradiographic study. J. Comp. Neurol. *298*, 431–442.

Banse, R., and Scherer, K.R. (1996). Acoustic profiles in vocal emotion expression. J. Pers. Soc. Psychol. *70*, 614–636.

Bartolomei, S., Nigro, F., Gubellini, L., Semprini, G., Ciacci, S., Hoffman, J.R., and Merni, F. (2018). Acute Effects of Ammonia Inhalants on Strength and Power Performance in Trained Men. J. Strength Cond. Res. *32*, 244–247.

Beierholm, U., Guitart-Masip, M., Economides, M., Chowdhury, R., Düzel, E., Dolan, R., and Dayan, P. (2013). Dopamine modulates reward-related vigor. Neuropsychopharmacology *38*, 1495–1503.

Berardelli, A., Rothwell, J.C., Thompson, P.D., and Hallett, M. (2001). Pathophysiology of bradykinesia in Parkinson's disease. Brain *124*, 2131–2146.

Berg, R.W., Friedman, B., Schroeder, L.F., and Kleinfeld, D. (2005). Activation of Nucleus Basalis Facilitates Cortical Control of a Brain Stem Motor Program. J. Neurophysiol. *94*, 699–711.

Berger-Sweeney, J., Heckers, S., Mesulam, M., Wiley, R., Lappi, D., and Sharma, M. (1994). Differential effects on spatial navigation of immunotoxin-induced cholinergic lesions of the medial septal area and nucleus basalis magnocellularis. J. Neurosci. *14*, 4507–4519.

Bertelson, P. (1967). The Time Course of Preparation*. Q. J. Exp. Psychol. *19*, 272–279.

Bishop, D.T., Karageorghis, C.I., and Kinrade, N.P. (2009). Effects of Musically-Induced Emotions on Choice Reaction Time Performance. Sport Psychol. *23*, 59–76.

Bonanni, L., Thomas, A., and Onofrj, M. (2010). Paradoxical kinesia in parkinsonian patients surviving earthquake. Mov. Disord. *25*, 1302–1304.

Bouman, D., Stins, J.F., and Beek, P.J. (2015). Arousal and exposure duration affect forward step initiation. Front. Psychol. *6*, 1667.

Buchman, A.S., Wilson, R.S., Boyle, P.A., Bienias, J.L., and Bennett, D.A. (2007). Grip Strength and the Risk of Incident Alzheimer's Disease. Neuroepidemiology *29*, 66–73.

Buzsaki, G., Bickford, R.G., Ponomareff, G., Thal, L.J., Mandel, R., and Gage, F.H. (1988). Nucleus basalis and thalamic control of neocortical activity in the freely moving rat. J. Neurosci. *8*, 4007–4026.

Chen, N., Sugihara, H., and Sur, M. (2015). An acetylcholine-activated microcircuit drives temporal dynamics of cortical activity. Nat. Neurosci. *18*, 892–902.

Cheney, P.D., and Fetz, E.E. (1980). Functional classes of primate corticomotoneuronal cells and their relation to active force. J. Neurophysiol. *44*, 773–791.

Churchland, M.M., Yu, B.M., Cunningham, J.P., Sugrue, L.P., Cohen, M.R., Corrado, G.S., Newsome, W.T., Clark, A.M., Hosseini, P., Scott, B.B., et al. (2010). Stimulus onset quenches neural variability: a widespread cortical phenomenon. Nat. Neurosci. *13*, 369–378.

Cooper, B.G., and Goller, F. (2006). Physiological Insights Into the Social-Context-Dependent Changes in the Rhythm of the Song Motor Program. J. Neurophysiol. *95*, 3798–3809.

Dai, T., Liu, J., Sahgal, V., Brown, R., and Yue, G. (2001). Relationship between muscle output and functional MRI-measured brain activation. Exp. Brain Res. *140*, 290–300.

Darshan, R., Wood, W.E., Peters, S., Leblois, A., and Hansel, D. (2017). A canonical neural mechanism for behavioral variability. Nat. Commun. *8*, 15415.

Deco, G., and Hugues, E. (2012). Neural Network Mechanisms Underlying Stimulus Driven Variability Reduction. PLoS Comput. Biol. *8*, e1002395.

Desai, N.S. (2006). Synaptic Bombardment Modulates Muscarinic Effects in Forelimb Motor Cortex. J. Neurosci. *26*, 2215–2226.

DiGirolamo, G.J., Patel, N., and Blaukopf, C.L. (2016). Arousal facilitates involuntary eye movements. Exp. Brain Res. *234*, 1967–1976.

Dudman, J.T., and Krakauer, J.W. (2016). The basal ganglia: from motor commands to the control of vigor. Curr. Opin. Neurobiol. *37*, 158–166.

Eckenstein, F.P., Baughman, R.W., and Quinn, J. (1988). An anatomical study of cholinergic innervation in rat cerebral cortex. Neuroscience *25*, 457–474.

Eggermann, E., Kremer, Y., Crochet, S., and Petersen, C.C.H. (2014). Cholinergic Signals in Mouse Barrel Cortex during Active Whisker Sensing. Cell Rep. *9*, 1654–1660.

Evarts, E. V (1968). Relation of pyramidal tract activity to force exerted during voluntary movement. J. Neurophysiol. *31*, 14–27.

Fairbanks, G., and Pronovost, W. (1938). VOCAL PITCH DURING SIMULATED EMOTION. Science *88*, 382–383.

Ferris, S.H., and Farlow, M. (2013). Language impairment in Alzheimer's disease and benefits of acetylcholinesterase inhibitors. Clin. Interv. Aging *8*, 1007–1014.

Francis, P.T., Palmer, A.M., Snape, M., and Wilcock, G.K. (1999). The cholinergic hypothesis of Alzheimer's disease: a review of progress. J. Neurol. Neurosurg. Psychiatry *66*, 137–147.

Fu, Y., Tucciarone, J.M., Espinosa, J.S., Sheng, N., Darcy, D.P., Nicoll, R.A., Huang, Z.J., and

Stryker, M.P. (2014). A cortical circuit for gain control by behavioral state. Cell *156*, 1139–1152.

Galani, R., Lehmann, O., Bolmont, T., Aloy, E., Bertrand, F., Lazarus, C., Jeltsch, H., and Cassel, J.-C. (2002). Selective immunolesions of CH4 cholinergic neurons do not disrupt spatial memory in rats. Physiol. Behav. *76*, 75–90.

Garst-Orozco, J., Babadi, B., and Ölveczky, B.P. (2014). A neural circuit mechanism for regulating vocal variability during song learning in zebra finches. Elife *3*.

Gharbawie, O.A., and Whishaw, I.Q. (2003). Cholinergic and serotonergic neocortical projection lesions given singly or in combination cause only mild impairments on tests of skilled movement in rats: evaluation of a model of dementia. Brain Res. *970*, 97–109.

Glaze, C.M., Castelino, C.B., Bibu, S.P., Yau, E., and Schmidt, M.F. (2017). Regulation of vocal precision by local noradrenergic modulation of a motor nucleus. BioRxiv 218479.

Glickstein, M., and Stein, J. (1991). Paradoxical movement in Parkinson's disease. Trends Neurosci. *14*, 480–482.

Goard, M., and Dan, Y. (2009). Basal forebrain activation enhances cortical coding of natural scenes. Nat. Neurosci. *12*, 1444–1449.

Goldman, W.P., Baty, J.D., Buckles, V.D., Sahrmann, S., and Morris, J.C. (1999). Motor dysfunction in mildly demented AD individuals without extrapyramidal signs. Neurology *53*, 956–962.

Goller, F., and Riede, T. (2013). Integrative physiology of fundamental frequency control in birds. J. Physiol. *107*, 230–242.

Gu, Z., Alexander, G.M., Dudek, S.M., and Yakel, J.L. (2017). Hippocampus and Entorhinal Cortex Recruit Cholinergic and NMDA Receptors Separately to Generate Hippocampal Theta

Oscillations. Cell Rep. *21*, 3585–3595.

Hahnloser, R.H.R., Kozhevnikov, A.A., and Fee, M.S. (2002). An ultra-sparse code underliesthe generation of neural sequences in a songbird. Nature *419*, 65–70.

Hamaguchi, K., Tanaka, M., and Mooney, R. (2016). A Distributed Recurrent Network Contributes to Temporally Precise Vocalizations. Neuron *91*, 680–693.

Hampton, C.M., Sakata, J.T., and Brainard, M.S. (2009). An Avian Basal Ganglia-Forebrain Circuit Contributes Differentially to Syllable Versus Sequence Variability of Adult Bengalese Finch Song. J. Neurophysiol. *101*, 3235–3245.

Hangya, B., Ranade, S.P., Lorenc, M., and Kepecs, A. (2015). Central Cholinergic Neurons Are Rapidly Recruited by Reinforcement Feedback. Cell *162*, 1155–1168.

Hennequin, G., Ahmadian, Y., Rubin, D.B., Lengyel, M., and Miller, K.D. (2018). The Dynamical Regime of Sensory Cortex: Stable Dynamics around a Single Stimulus-Tuned Attractor Account for Patterns of Noise Variability. Neuron *98*, 846-860.e5.

Herrero, J.L., Roberts, M.J., Delicato, L.S., Gieselmann, M.A., Dayan, P., and Thiele, A. (2008). Acetylcholine contributes through muscarinic receptors to attentional modulation in V1. Nature *454*, 1110–1114.

Howe, W.M., Gritton, H.J., Lusk, N.A., Roberts, E.A., Hetrick, V.L., Berke, J.D., and Sarter, M. (2017). Acetylcholine Release in Prefrontal Cortex Promotes Gamma Oscillations and Theta–Gamma Coupling during Cue Detection. J. Neurosci. *37*, 3215–3230.

James, L.S., and Sakata, J.T. (2015). Predicting plasticity: acute context-dependent changes to vocal performance predict long-term age-dependent changes. J. Neurophysiol. *114*, 2328–2339.

Kao, M.H., and Brainard, M.S. (2006). Lesions of an Avian Basal Ganglia Circuit Prevent Context-Dependent Changes to Song Variability. J. Neurophysiol. *96*, 1441–1455.

Kao, M.H., Doupe, A.J., and Brainard, M.S. (2005). Contributions of an avian basal ganglia–forebrain circuit to real-time modulation of song. Nature *433*, 638–643.

Karageorghis, C.I., Drew, K.M., and Terry, P.C. (1996). Effects of Pretest Stimulative and Sedative Music on Grip Strength. Percept. Mot. Skills *83*, 1347–1352.

Kaufman, M.T., Churchland, M.M., Ryu, S.I., and Shenoy, K. V (2014). Cortical activity in the null space: permitting preparation without movement. Nat. Neurosci. *17*, 440–448.

Leblois, A., Wendel, B.J., and Perkel, D.J. (2010). Striatal dopamine modulates basal ganglia output and regulates social context-dependent behavioral variability through D1 receptors. J. Neurosci. *30*, 5730–5743.

Lee, S.-H., and Dan, Y. (2012). Neuromodulation of brain states. Neuron *76*, 209–222.

Leinonen, L., Hiltunen, T., Linnankoski, I., and Laakso, M.-L. (1997). Expression of emotional–motivational connotations with a one-word utterance. J. Acoust. Soc. Am. *102*, 1853–1863.

Long, M.A., and Fee, M.S. (2008). Using temperature to analyse temporal dynamics in the songbird motor pathway. Nature *456*, 189–194.

Lovett-Barron, M., Andalman, A.S., Allen, W.E., Vesuna, S., Kauvar, I., Burns, V.M., and Deisseroth, K. (2017). Ancestral Circuits for the Coordinated Modulation of Brain State. Cell *171*, 1411-1423.e17.

Lynch, G.F., Okubo, T.S., Hanuschkin, A., Hahnloser, R.H.R., and Fee, M.S. (2016). Rhythmic Continuous-Time Coding in the Songbird Analog of Vocal Motor Cortex. Neuron *90*, 877–892.

Manohar, S.G., Chong, T.T.-J., Apps, M.A.J., Batla, A., Stamelou, M., Jarman, P.R., Bhatia, K.P., and Husain, M. (2015). Reward Pays the Cost of Noise Reduction in Motor and Cognitive Control. Curr. Biol. *25*, 1707–1716.

Marshall, J.F., Levitan, D., and Stricker, E.M. (1976). Activation-induced restoration of

sensorimotor functions in rats with dopamine-depleting brain lesions. J. Comp. Physiol. Psychol. *90*, 536–546.

Mastrogiuseppe, F., and Ostojic, S. (2018). Linking Connectivity, Dynamics, and Computations in Low-Rank Recurrent Neural Networks. Neuron *99*, 609-623.e29.

Matheson, L.E., Sun, H., and Sakata, J.T. (2016). Forebrain circuits underlying the social modulation of vocal communication signals. Dev. Neurobiol. *76*, 47–63.

Mazzoni, P., Hristova, A., and Krakauer, J.W. (2007). Why Don't We Move Faster? Parkinson's Disease, Movement Vigor, and Implicit Motivation. J. Neurosci. *27*, 7105–7116.

McGinley, M.J., David, S.V., and McCormick, D.A. (2015). Cortical Membrane Potential Signature of Optimal States for Sensory Signal Detection. Neuron *87*, 179–192.

McKinney, M., Coyle, J.T., and Hedreen, J.C. (1983). Topographic analysis of the innervation of the rat neocortex and hippocampus by the basal forebrain cholinergic system. J. Comp. Neurol. *217*, 103–121.

Metherate, R., Cox, C.L., and Ashe, J.H. (1992). Cellular bases of neocortical activation: modulation of neural oscillations by the nucleus basalis and endogenous acetylcholine. J. Neurosci. *12*, 4701–4711.

Miller, M.N., Cheung, C.Y.J., and Brainard, M.S. (2017). Vocal learning promotes patterned inhibitory connectivity. Nat. Commun. *8*, 2105.

Mitra, P., and Bokil, H. (2007). Observed Brain Dynamics (Oxford University Press).

Nebes, R.D., and Brady, C.B. (1993). Phasic and tonic alertness in Alzheimer's disease. Cortex. *29*, 77–90.

Nelson, A., and Mooney, R. (2016). The Basal Forebrain and Motor Cortex Provide Convergent yet Distinct Movement-Related Inputs to the Auditory Cortex. Neuron *90*, 635–648.

Panigrahi, B., Martin, K.A., Li, Y., Graves, A.R., Vollmer, A., Olson, L., Mensh, B.D., Karpova, A.Y., and Dudman, J.T. (2015). Dopamine Is Required for the Neural Representation and Control of Movement Vigor. Cell *162*, 1418–1430.

Pinto, L., Goard, M.J., Estandian, D., Xu, M., Kwan, A.C., Lee, S.-H., Harrison, T.C., Feng, G., and Dan, Y. (2013). Fast modulation of visual perception by basal forebrain cholinergic neurons. Nat. Neurosci. *16*, 1857–1863.

Quiroga, R.Q., Nadasdy, Z., and Ben-Shaul, Y. (2004). Unsupervised Spike Detection and Sorting with Wavelets and Superparamagnetic Clustering. Neural Comput. *16*, 1661–1687.

Raghanti, M.A., Stimpson, C.D., Marcinkiewicz, J.L., Erwin, J.M., Hof, P.R., and Sherwood, C.C. (2008). Cholinergic innervation of the frontal cortex: Differences among humans, chimpanzees, and macaque monkeys. J. Comp. Neurol. *506*, 409–424.

Rajan, K., Abbott, L.F., and Sompolinsky, H. (2010). Stimulus-dependent suppression of chaos in recurrent neural networks. Phys. Rev. E *82*, 011903.

Reimer, J., McGinley, M.J., Liu, Y., Rodenkirch, C., Wang, Q., McCormick, D.A., and Tolias, A.S. (2016). Pupil fluctuations track rapid changes in adrenergic and cholinergic activity in cortex. Nat. Commun. *7*, 13289.

Ryan, S.M., and Arnold, A.P. (1981). Evidence for cholinergic participation in the control of bird song: Acetylcholinesterase distribution and muscarinic receptor autoradiography in the zebra finch brain. J. Comp. Neurol. *202*, 211–219.

Saar, S., and Mitra, P.P. (2008). A Technique for Characterizing the Development of Rhythms in Bird Song. PLoS One *3*, e1461.

Sakata, J.T., and Brainard, M.S. (2008). Online Contributions of Auditory Feedback to Neural Activity in Avian Song Control Circuitry. J. Neurosci. *28*, 11378–11390.

Sakata, J.T., Hampton, C.M., and Brainard, M.S. (2008). Social Modulation of Sequence and Syllable Variability in Adult Birdsong. J. Neurophysiol. *99*, 1700–1711.

Shea, S.D., and Margoliash, D. (2003). Basal Forebrain Cholinergic Modulation of Auditory Activity in the Zebra Finch Song System. Neuron *40*, 1213–1226.

Shea, S.D., Koch, H., Baleckaitis, D., Ramirez, J.-M., and Margoliash, D. (2010). Neuron-Specific Cholinergic Modulation of a Forebrain Song Control Nucleus. J. Neurophysiol. *103*, 733–745.

da Silva, J.A., Tecuapetla, F., Paixão, V., and Costa, R.M. (2018). Dopamine neuron activity before action initiation gates and invigorates future movements. Nature *554*, 244–248.

Sober, S.J., Wohlgemuth, M.J., and Brainard, M.S. (2008). Central contributions to acoustic variation in birdsong. J. Neurosci. *28*, 10370–10379.

Spraker, M.B., Yu, H., Corcos, D.M., and Vaillancourt, D.E. (2007). Role of Individual Basal Ganglia Nuclei in Force Amplitude Generation. J. Neurophysiol. *98*, 821–834.

Srivastava, K.H., Elemans, C.P.H., and Sober, S.J. (2015). Multifunctional and Context-Dependent Control of Vocal Acoustics by Individual Muscles. J. Neurosci. *35*, 14183–14194.

Stepanek, L., and Doupe, A.J. (2010). Activity in a Cortical-Basal Ganglia Circuit for Song Is Required for Social Context-Dependent Vocal Variability. J. Neurophysiol. *104*, 2474–2486.

Stroud, J.P., Porter, M.A., Hennequin, G., and Vogels, T.P. (2018). Motor primitives in space and time via targeted gain modulation in cortical networks. Nat. Neurosci. *21*, 1774–1783.

Summerside, E.M., Shadmehr, R., and Ahmed, A.A. (2018). Vigor of reaching movements: reward discounts the cost of effort. J. Neurophysiol. *119*, 2347–2357.

Suri, H., and Rajan, R. (2018). Distance-dependent changes in courtship song amplitude reflect song state changes. BioRxiv 277210.

Takikawa, Y., Kawagoe, R., Itoh, H., Nakahara, H., and Hikosaka, O. (2002). Modulation of saccadic eye movements by predicted reward outcome. Exp. Brain Res. *142*, 284–291.

Thiele, A. (2013). Muscarinic Signaling in the Brain. Annu. Rev. Neurosci. *36*, 271–294.

Ungerstedt, U. (1971). Adipsia and Aphagia after 6-Hydroxydopamine Induced Degeneration of the Nigro-striatal Dopamine System. Acta Physiol. Scand. *82*, 95–122.

Vandecasteele, M., Varga, V., Berényi, A., Papp, E., Barthó, P., Venance, L., Freund, T.F., and Buzsáki, G. (2014). Optogenetic activation of septal cholinergic neurons suppresses sharp wave ripples and enhances theta oscillations in the hippocampus. Proc. Natl. Acad. Sci. U. S. A. *111*, 13535–13540.

Vitrac, C., and Benoit-Marand, M. (2017). Monoaminergic Modulation of Motor Cortex Function. Front. Neural Circuits *11*, 72.

Wardle, M.C., Treadway, M.T., Mayo, L.M., Zald, D.H., and de Wit, H. (2011). Amping up effort: effects of d-amphetamine on human effort-based decision-making. J. Neurosci. *31*, 16597–16602.

Watson, J.T., Adkins-Regan, E., Whiting, P., Lindstrom, J.M., and Podleski, T.R. (1988). Autoradiographic localization of nicotinic acetylcholine receptors in the brain of the zebra finch (Poephila guttata). J. Comp. Neurol. *274*, 255–264.

Wood, W.E., Osseward, P.J., Roseberry, T.K., and Perkel, D.J. (2013). A Daily Oscillation in the Fundamental Frequency and Amplitude of Harmonic Syllables of Zebra Finch Song. PLoS One *8*, e82327.

Xu-Wilson, M., Zee, D.S., and Shadmehr, R. (2009). The intrinsic value of visual information affects saccade velocities. Exp. Brain Res. *196*, 475–481.

Yttri, E.A., and Dudman, J.T. (2016). Opponent and bidirectional control of movement velocity

in the basal ganglia. Nature *533*, 402–406.

Zhang, Y.S., Wittenbach, J.D., Jin, D.Z., and Kozhevnikov, A.A. (2017). Temperature

Manipulation in Songbird Brain Implicates the Premotor Nucleus HVC in Birdsong Syntax. J.

Neurosci. *37*, 2600–2611.

Zuschratter, W., and Scheich, H. (1990). Distribution of choline acetyltransferase and

acetylcholinesterase in the vocal motor system of zebra finches. Brain Res. *513*, 193–201.

Publishing Agreement

It is the policy of the University to encourage the distribution of all theses, dissertations, and manuscripts. Copies of all UCSF theses, dissertations, and manuscripts will be routed to the library via the Graduate Division. The library will make all theses, dissertations, and manuscripts accessible to the public and will preserve these to the best of their abilities, in perpetuity.

Please sign the following statement:

I hereby grant permission to the Graduate Division of the University of California, San Francisco to release copies of my thesis, dissertation, or manuscript to the Campus Library to provide access and preservation, in whole or in part, in perpetuity.

_____   8/30/2019
                                             _____
Author Signature   Date